JGR Earth Surface

RESEARCH ARTICLE
10.1029/2021JF006231

Key Points:
- Coastal sedimentary strata under effective stresses of >10 kPa, particularly organic-rich sediments, are likely substantially compacted
- A large portion of the compaction in such organic-rich strata occurs in the top 1–3 m and the first 100–500 years after deposition
- Though deposition in deltaic wetlands may drive compaction, river diversions in the Mississippi Delta will likely yield net elevation gain

Supporting Information:
Supporting Information may be found in the online version of this article.

Correspondence to:
M. E. Keogh,
mkeogh@uoregon.edu

Citation:
Keogh, M. E., Törnqvist, T. E., Kolker, A. S., Erkens, G., & Bridgeman, J. G. (2021). Organic matter accretion, shallow subsidence, and river delta sustainability. *Journal of Geophysical Research: Earth Surface*, *126*, e2021JF006231. https://doi.org/10.1029/2021JF006231

Received 26 APR 2021
Accepted 27 OCT 2021

Organic Matter Accretion, Shallow Subsidence, and River Delta Sustainability

Molly E. Keogh[1,2], Torbjörn E. Törnqvist[1], Alexander S. Kolker[3], Gilles Erkens[4,5], and Jonathan G. Bridgeman[1]

[1]Department of Earth and Environmental Sciences, Tulane University, New Orleans, LA, USA, [2]Department of Earth Sciences, University of Oregon, Eugene, OR, USA, [3]Louisiana Universities Marine Consortium, Chauvin, LA, USA, [4]Deltares Research Institute, Utrecht, The Netherlands, [5]Department of Physical Geography, Utrecht University, Utrecht, The Netherlands

Abstract Globally, mineral sediment supply to deltaic wetlands has generally decreased so these wetlands increasingly rely on accretion of organic matter to keep pace with relative sea-level rise (RSLR). Because organic-rich sediments tend to be more compressible than mineral-dominated sediments, deltaic wetland strata are vulnerable to compaction and drowning. Using an unprecedented data set of almost 3,000 discrete bulk density and organic-matter measurements, we examine organic-rich facies from coastal Louisiana to quantify the thickness lost to compaction and investigate whether sediments are able to maintain sufficient volume for the associated wetlands to keep pace with RSLR. We find that organic content as well as overburden thickness and density (which together determine effective stress) strongly control sediment compaction. Most compaction occurs in the top 1–3 m and within the first 100–500 years after deposition. In settings with thick peat beds, successions up to 14 m thick have been compacted by up to ~50%. We apply geotechnical modeling to examine the balance between elevation gained from accretion and elevation lost to compaction due to renewed sediment deposition over a 100-year timescale. Wetlands overlying mineral-dominated lithologies may support the weight of deposition and allow net elevation gain. Model results show that reintroduction of sediment to a representative Mississippi Delta wetland site will likely cause another ~0.35–1.14 m of compaction but leave a net elevation gain of ~0.01–1.75 m, depending on the sediment delivery rate and stiffness of underlying strata.

Plain Language Summary River deltas constitute some of the most valuable but also most vulnerable environments on the planet. Their elevation right above sea level is controlled by a delicate balance between sediment deposition and compaction. If sediment delivery is reduced due to dam construction in the hinterland, for example, sedimentation rates decrease. Continued sediment compaction may prevent deltas from keeping up with sea-level rise and increase the risk of drowning. In this study, we investigate the magnitude of compaction that occurs in deltaic wetlands. We find that highly organic sediments are particularly susceptible to compaction, especially when they are buried by sand or mud. As a result, deltaic wetlands cannot rely on organic matter alone to keep pace with sea-level rise. These findings are relevant to delta restoration efforts where sediment is reintroduced to previously isolated wetlands to combat wetland loss. For restoration to be successful, elevation gained from new sediment deposition must outpace elevation lost to compaction. The portion of the Mississippi Delta where this restoration strategy has been planned indicates potentially favorable conditions for land building, provided that sediment loads are high, and the underlying material is strong and mineral rich.

1. Introduction

River deltas serve as critical nodes in the global water-energy-food nexus. They host large and rapidly growing populations (Edmonds et al., 2020) with associated economic assets, and many deltas provide important ecosystem goods and services. Thus, delta sustainability is a critical issue, and it is widely recognized that maintaining deltaic plains in the face of accelerating relative sea-level rise (RSLR) is a major priority that will become increasingly daunting in the future (e.g., Day et al., 2016; Hoitink et al., 2020; Nienhuis et al., 2020). On many deltaic plains, mineral sediment supply has decreased dramatically since the mid-twentieth century, largely due to the construction of dams, artificial levees, and other flood-control infrastructure (e.g., Giosan et al., 2014; Syvitski et al., 2005; Weston, 2014), a trend that is expected to continue in the 21st century (Dunn et al., 2019). In the Yangtze and Mississippi rivers, for example, dams have reduced the suspended sediment concentration by

>40% (Yang et al., 2006) and >60% (Sanks et al., 2020), respectively. Globally, 40% of river discharge is intercepted by large-capacity reservoirs (Vörösmarty et al., 2003), which have trapped more than 100 billion tons of sediment (Syvitski et al., 2005). Exacerbating the problem, artificial levees prevent overbank deposition and the remaining sediment from reaching deltaic plains, which commonly host extensive wetlands (Giosan et al., 2014). These coastal wetlands are usually distal from the main channel(s) and play an important role in trapping sediment, both in terms of areal extent and volume. Although these wetlands may receive some mineral sediment through tidal exchange and storms (e.g., Nyman et al., 1994), sediment import from the coastal ocean is generally not sufficient to maintain them in the face of RSLR and erosion (e.g., Chant et al., 2021). With reduced input of mineral matter (MM), deltaic wetlands must rely to a larger extent on the accretion of organic matter (OM) to keep pace with accelerating RSLR. If RSLR exceeds vertical accretion, wetlands eventually drown and convert to tidal flats or open water.

Previous work has debated the relative importance of MM and OM in delta accretion (e.g., Edmonds, 2012; Lorenzo-Trueba et al., 2012). Because organic-rich sediments, and especially peats, are typically more compressible than their MM-dominated counterparts (e.g., Kaye & Barghoorn, 1964), coastal wetlands are vulnerable to compaction-driven subsidence and conversion to open water. Furthermore, Day et al. (2011) found that soil strength is higher in marshes with riverine MM input compared to marshes with high OM content that lack riverine input. However, MM-dominated deltaic muds are also highly compressible (e.g., Fisk et al., 1954; Minderhoud et al., 2018; Zoccarato et al., 2018) and may be at least as compressible as organic-rich sediments in some cases (e.g., Chamberlain et al., 2021).

Despite its compressibility, OM can be an important component of vertical accretion, at least over short timescales. For example, in fresh, intermediate, and brackish marshes of the Mississippi Delta, Nyman et al. (1990) found that in the top 38–50 cm, OM occupies 27%–198% more volume than MM. This is likely universally true for unconsolidated peats because of the low OM density compared to MM. Turner (1997) suggested that OM accretion alone may be sufficient for Mississippi Delta wetlands to keep pace with RSLR. Subsequently, Turner et al. (2002) claimed that at RSLR rates of $\geq$0.2 cm yr^{-1}, salt marshes may survive on OM accretion alone. Nyman et al. (2006) found that in the top 45–55 cm, vertical accretion is more closely correlated with OM than MM accretion rates. In a review of 76 tidal freshwater marshes in North America and Europe, including both OM- and MM-dominated systems, Neubauer (2008) quantified the relative importance of OM in the top ~30 cm and concluded that, on average, 62% of marsh vertical accretion is due to OM and the remaining 38% due to MM. Most recently, Sanks et al. (2020) showed that OM accretion plays a substantial role in the ability of the Mississippi Delta to keep up with RSLR over the past decade. Mariotti et al. (2020) demonstrated the importance of OM accretion via mud deposition, where OM is mixed with MM and imported into a marsh, rather than produced *in situ* from plant remains. They showed that in Louisiana salt and brackish marshes, OM-rich mud contributes up to 60% of total vertical accretion.

Sediment bulk density (herein we use dry bulk density, with units of g dry material per cm^3 wet volume) is known to increase with burial depth (and thus also with time) due to compaction (e.g., Baldwin, 1971; Van Asselen et al., 2011). However, details about the bulk density versus depth relationship are not well known. Although there is an extensive literature on sediment compaction over large (10^3 m) depth intervals and long (>10^6 yr) timescales from the hydrocarbon industry (e.g., Baldwin, 1971; Rieke & Chilingarian, 1974), comparatively little is known about the compaction of shallower (10^{-2} to 10^1 m) deposits over 10^0–10^3 yr timescales. Here we address this knowledge gap, which is key to understanding the evolution and resilience of modern deltas and associated coastal wetland environments, by investigating shallow compaction with a new data set that is unprecedented in size, offering exceptionally high depth-time resolution.

Near the surface (0–10 cm depth), coastal wetland sediments typically possess very low bulk densities, generally within the range of 0.1–0.6 g cm^{-3} (e.g., Giosan et al., 2013; Keogh et al., 2019; Marsh et al., 1999; Nyman et al., 2006). At greater depth (>2 m), the bulk density of MM-dominated deposits is commonly in the range of 1.0–1.5 g cm^{-3} (e.g., Brevik & Homburg, 2004; Kuecher et al., 1993). Using data from Jankowski et al. (2017), Keogh and Törnqvist (2019) found that the majority of sediment compaction in the Mississippi Delta occurs in the shallowest 5 m, suggesting that sediment bulk density increases rapidly with initial burial. Here we examine this relationship in more detail and find that the interval of most rapid compaction may be restricted to even shallower depths.

10.1029/2021JF006231

The intricate connection between OM, accretion, and subsidence is of particular importance due to the increasing interest in resuming natural processes to restore deltaic plains and related coastal environments. These restoration efforts involve reintroducing mineral sediment to enable land building in areas that have been disconnected from the sediment source, usually due to flood-protection engineering (e.g., Auerbach et al., 2015; Calvo-Cubero et al., 2013; Giosan et al., 2013; Temmerman & Kirwan, 2015; Van der Deijl et al., 2018). To date, little attention has been given to how the loading associated with the introduction of mineral sediment may affect underlying, organic-rich strata in terms of sediment compaction (a notable exception is the study by Nienhuis et al., 2018). Put differently, the goal of accomplishing elevation gain on deltaic plains will not necessarily be met if compaction rates are high.

Using an extensive and novel data set compiled from multiple sources (and made wholly available to the research community for future use), we combine sediment core data and modeling to examine volumetric changes of organic-rich facies in the Mississippi Delta. Herein, organic-rich (or OM-dominated) sediments are defined as those with ≥5% OM content. Material with ≥26% OM content is defined as peat. Sediments with <5% OM content are considered MM-dominated. We identify the depth range and timescale over which most sediment compaction occurs and predict future compaction-driven surface-elevation change. By comparing the bulk density of sediments at the surface with similar deposits buried at depth, we quantify the thickness lost to compaction and investigate how much RSLR organic-rich sediments and peats can offset. To better understand the role of OM in delta accretion, we test the hypothesis that the bulk density of OM increases non-linearly with burial depth and overburden weight (i.e., effective stress), with a high compaction rate during initial burial that decreases asymptotically to a much slower and more constant rate at depth. As a result, OM accretion in the Mississippi Delta may be sufficient for most wetlands to keep pace with RSLR (currently 13 ± 9 mm/yr as measured with respect to the wetland surface; Jankowski et al., 2017) in the short term (years to decades) but not over longer timescales (centuries to millennia) as compaction proceeds (cf., Törnqvist et al., 2021) and the rate of global sea-level rise accelerates (e.g., CPRA, 2017; Fox-Kemper et al., 2021; Oppenheimer et al., 2019).

Our findings also have implications for reconstructions of RSLR based on the stratigraphic record from deltaic and related coastal environments. Organic-rich strata feature prominently in such investigations (e.g., Khan et al., 2019) but they do so under the assumption that compaction is either negligible or that it can be corrected for. Our new data set can serve as a starting point for renewed efforts to address this important issue by means of geotechnical modeling. This is particularly important for studies of late Holocene sea-level change that require sub-decimeter scale vertical resolution and where compaction effects may be significant (e.g., Brain et al., 2017; Tam et al., 2018).

2. Data

To test our hypothesis, we synthesized data from five sources consisting of 330 sediment cores previously collected in coastal Louisiana, USA. Data associated with each core include dry bulk density, loss-on-ignition (LOI, a measure of OM content), and geochronology; these data are summarized in Table S1. Core locations are shown in Figure 1 and Table S2.

2.1. Coastwide Reference Monitoring System Cores

The majority of the cores used in this analysis ($n = 264$) were collected across the Louisiana coast within the context of the Coastwide Reference Monitoring System (CRMS; CPRA, 2018; Steyer et al., 2003). At each CRMS station, three 24-cm cores were obtained immediately following site construction. Most CRMS sites were established between 2006 and 2010. Cores were collected by hand and analyzed as described in Folse et al. (2012). CRMS cores included in our analysis have dry bulk density and LOI measurements every 4 cm (for a total of six increments per core) and modern vertical accretion rates from feldspar marker horizons as calculated by Jankowski et al. (2017) based on at least six years of data between 2006 and 2015. Note that the vertical accretion rates postdate the time interval covered by the cores. For each sample interval, dry bulk density and LOI measurements from each of the triplicate cores were averaged to produce a single value with an error term of one standard deviation. Linear extrapolation of modern vertical accretion rates was used to estimate the age of buried sediments, which may result in an underestimation of sample ages. The validity of this and other assumptions is discussed in the Supporting Information S1.

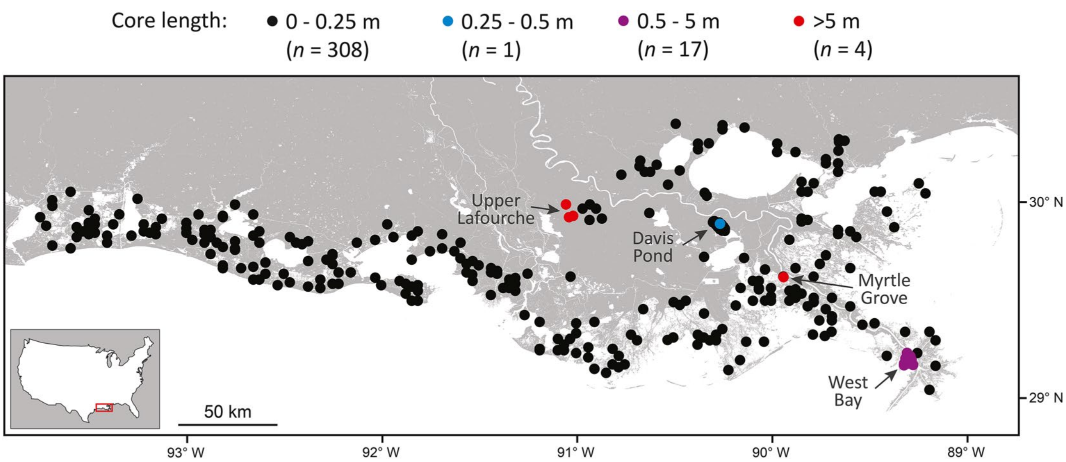

Figure 1. Location of 330 sediment cores across the Louisiana coast that were used for analysis. Colors correspond to core length.

2.2. Davis Pond Cores

Short (0.05–0.5 m) hand cores ($n = 45$) were collected by Keogh et al. (2019) in 2015 and 2016 in the receiving basin of the Davis Pond Freshwater Diversion, adjacent to the Mississippi River ~30 river km upstream of New Orleans. Data for five of these cores are previously unpublished (Table S1). Dry bulk density, LOI, and activity of the radioisotope ^{7}Be were measured in 1-cm-increments for the top 5 cm and in 5-cm-increments below that to the base of the core. ^{7}Be activity and vertical accretion rates provided in Keogh et al. (2019) were used to estimate the age of buried sediments.

2.3. West Bay Cores

Seventeen vibracores ~3–5 m in length were collected in 2014 in the receiving basin of the West Bay Mississippi River Diversion, which is located ~7 km upriver from Head of Passes near the mouth of the Mississippi River. In these cores, dry bulk density, LOI, and activities of the radioisotopes ^{210}Pb and ^{137}Cs were measured in 10-cm intervals to estimate the age of buried sediments (previously unpublished data; Table S1). Sediment compaction, which commonly occurs during the collection of vibracores, ranged from 3%-13% of total core length. Core length and bulk density measurements were corrected for coring-related compaction, assuming that compaction occurred uniformly throughout the cores.

2.4. Upper Lafourche Cores

Three longer (~12–14 m) cores were collected with a Geoprobe in the upper Bayou Lafourche area near Paincourtville and Napoleonville, Louisiana, in 2013. Dry bulk density and LOI data are available in ~10-cm depth intervals beginning 0.6, 3.7, and 7.8 m below the surface (Jankowski, 2018). At shallower depths, bulk density and LOI values were estimated based on sediment texture descriptions made in the field. Bulk density values were calculated using subsamples with a known volume (Jankowski, 2018). The LOI data are previously unpublished and were provided by K. L. Jankowski (Table S1). The ages of buried sediments were estimated using ^{14}C (Jankowski, 2018) and optically stimulated luminescence (OSL; Shen et al., 2015) dating of organic and mineral sediments, respectively.

2.5. Myrtle Grove Core

In 2016, a 38.7 m piston core was collected about 2 km from the Mississippi River and ~60 river km downstream of New Orleans. Dry bulk density and LOI measurements were made at 5–25 cm intervals (Bridgeman, 2018) beginning at a depth of 1.2 m. At shallower depths, bulk density and LOI values were estimated based on sediment texture descriptions. The bulk density values were calculated using subsamples of a known volume. ^{14}C and OSL ages were determined for organic and mineral sediments, respectively (Bridgeman, 2018).

3. Methods

We used 2,865 samples from the 330 sediment cores to assess the vulnerability of wetlands in coastal Louisiana to sediment compaction. In cores with vertical gaps between samples, measurements associated with each sample were assumed to also apply to the interval between samples (defined here as the sample interval). Sample intervals are separated at the mid-point between sample depths. For each sample interval, we calculated effective stress, decompacted dry bulk density, decompacted thickness, compaction ratio, and compaction rate. For cores longer than 0.5 m, values were integrated over the length of the entire core to calculate total compaction. Potential future compaction was evaluated using the geotechnical model D-Settlement.

3.1. Assessing Differences in Sampling Methods

In the Davis Pond and West Bay cores, dry bulk density was calculated using the measured LOI and estimated densities of 2.65 and 1.14 g cm^{-3} for MM and OM, respectively (Adams, 1973; DeLaune et al., 1983; Kolker et al., 2009; Morris et al., 2016). For all other cores used in this analysis, bulk density was directly measured using a subsampler with a known volume. A comparison of these two methods using data from the Myrtle Grove core produced a coefficient of determination of 0.86, indicating that the two methods produce comparable results (Equations S1–S3 and Figure S1 in Supporting Information S1). Note that for vertical gaps in cores where no subsamples were collected, LOI and bulk density were estimated based on sediment texture descriptions made in the field. Each LOI and bulk density estimate was used only to calculate effective stress and compaction for the specific core interval. Estimated values were otherwise excluded from the analysis (i.e., they are not included in the reference data set for uncompacted peat, used to derive the compaction equations, or included in the comparison of methods used to calculate bulk density [Figure S1 in Supporting Information S1]).

3.2. Calculating the Effective Stress

Using measured values of LOI (%) and dry bulk density (g cm^{-3}) and following the method described in Van Asselen et al. (2018), effective stress (σ', kPa) is calculated as,

$$\sigma' = \sigma - \mu \tag{1}$$

where σ is total stress and μ is porewater pressure. Details are provided in the Equations S4–S9 in Supporting Information S1. For the purposes of this calculation, we assume that the mineral component of all sediments is silty clay loam (35% clay, 55% silt, and 10% sand), a dominant sediment texture in Mississippi Delta overbank deposits (Esposito et al., 2017), and that the specific gravity of OM, clay, silt, and sand is 1.14, 2.70, 2.65, and 2.65 g cm^{-3}, respectively (Van Asselen et al., 2018, and references therein). Although the grain-size distribution is a required input for the calculation of effective stress (see Equations S4–S9 in Supporting Information S1), the specific gravities of sand, silt, and clay are similar enough that the assumed grain size distribution has essentially no impact on the resulting effective stress value, except for its relatively small influence on porosity (Equation S5 in Supporting Information S1). Furthermore, the mineral component in our samples is mud-dominated with minimal sand, so differential compaction due to grain size is unlikely to be a significant factor. All other assumptions, including values for pore volume and degree of saturation, are the same as those made in Van Asselen et al. (2018) and are described in the Supporting Information S1.

3.3. Calculating the Compaction Ratio

To calculate sediment compaction, we first identified a subset of near-surface sediment samples from our data set to be used as a reference for uncompacted material. This reference data set consists of samples in the uppermost 4 cm of all cores and includes 429 sample intervals from CRMS (n = 264), Davis Pond (n = 160), and West Bay (n = 5). These samples were assumed to be uncompacted. The relatively even spacing of the CRMS, Davis Pond, and West Bay sites across coastal Louisiana prevents the reference data set from being biased toward any one region.

The reference data set was then used to establish a relationship between uncompacted sediment bulk density (ρd_u) and OM content (LOI). Using the TableCurve 2D software (http://www.sigmaplot.co.uk/products/tablecurve2d/tablecurve2d.php), 75 equations were tested for goodness-of-fit. Only monotonic equations with no more than three parameters were considered. The resulting best-fit relationship and measured LOI values were then used to estimate the uncompacted bulk density of the remaining sediment samples at the time of deposition, before they were buried and subjected to loading.

Samples included in the reference data set were excluded from subsequent analyses. For the remainder of samples, a distinction was made between peat (LOI ≥26%) and sediments with LOI <26%. Above ∼26% OM content, mineral grains in a typical wetland sediment lose contact with one another and the sediment becomes supported by a matrix of OM (Den Haan & Kruse, 2007; Erkens et al., 2016).

Following Van Asselen (2011), the change in bulk density due to loading was used to calculate the uncompacted thickness of each sample interval (h_u):

$$h_u = \left(\rho d_c \ / \ \rho d_u\right) \times h_c \tag{2}$$

where h_c and ρd_c are the measured (compacted) interval thickness and bulk density, respectively. Because accretion and compaction occur simultaneously, h_u is a theoretical maximum thickness that may never have existed in reality. Compaction ratio ($C_{\%}$) was calculated as,

$$C_{\%} = 100 - \left[\left(h_u - h_c\right) / \ h_u \times 100\right] \tag{3}$$

where a $C_{\%}$ of 100% means that the sample is 100% of its original thickness (i.e., uncompacted). $C_{\%}$ values less than 100% indicate that compaction has occurred. Note that we calculate sediment compaction by length, following Van Asselen et al. (2018). In contrast, Van Asselen (2011) calculated compaction by volume, ignoring lateral strain.

3.4. Calculating the Compaction Rate

Based on the geochronology and vertical accretion rates available for each core, ages were calculated for all sediment intervals. Sediment intervals were assigned to one of five age bins, indicating the time elapsed since deposition: 0–10, 10–30, 30–100, 100–500, or 500–7,000 years. Each interval was normalized to a hypothetical 1-m-thick section and the sediment compaction rate (R, mm yr^{-1} m^{-1}) was calculated as,

$$R = \left(h_u - h_c\right) \times 1{,}000 \ / \ t \ / \ h_u \tag{4}$$

where t is the calculated age of the sample in years (see Table S1).

3.5. Calculating the Total Compaction

Following Van Asselen et al. (2018), total compaction per core (m) was calculated for all cores ≥0.5 m in length using the following equation:

$$C_{\text{tot}} = \sum h_u - \sum h_c \tag{5}$$

Additionally, we calculated the total compaction ratio as:

$$C_{\text{tot}\%} = 100 - \left[\left(\sum\left(h_u - h_c\right) / \sum h_u\right) \times 100\right] \tag{6}$$

3.6. Geotechnical Modeling

The Deltares geotechnical model D-Settlement (version 18.2, https://www.deltares.nl/en/software/d-settlement-2/) was used to predict sediment compaction (e.g., Peduto et al., 2017, 2020) that may occur as a result of future loading. The D-Settlement model is an engineering tool that is widely used for geotechnical projects in a variety of geographic settings worldwide, especially where accurate settlement calculations are required to ensure public safety (e.g., Abspoel et al., 2018; Hoefsloot, 2015; Peduto et al., 2017; Peduto et al., 2020; Visschedijk

Table 1
Lithologic Designations and Geotechnical Input Parameters Used for Modeling

Depth (m)	Lithology[a]	Unit weight above phreatic surface (kN m^{-3})	Unit weight below phreatic surface (kN m^{-3})	Vertical permeability (m s^{-1})	OCR	Weak stratigraphy			Stiff stratigraphy		
						RR	CR	Cα	RR	CR	Cα
0–1	Peat	11.00	10.50	5.00E-06	2.00	0.1533	0.4600	0.0230	0.1022	0.3067	0.0153
1–7	Silt loam	20.00	19.00	7.00E-06	1.25	0.0110	0.0329	0.0013	0.0077	0.0230	0.0009
7–10	Silty clay loam	20.00	19.00	1.03E-07	1.50	0.0307	0.0920	0.0037	0.0170	0.0511	0.0020
10–11.5	Sand	22.00	20.00	7.00E-06	1.00	0.0038	0.0115	0.0000	0.0019	0.0058	0.0000
11.5–35	Silty clay	19.00	18.00	7.00E-07	1.75	0.0383	0.1150	0.0046	0.0205	0.0614	0.0025
35–36.5	Sand	22.00	20.00	7.00E-06	1.00	0.0038	0.0115	0.0000	0.0019	0.0058	0.0000

Note. Geotechnical parameter values are from the Netherlands Standardization Institute (2006). Details are provided in Table S3 in Supporting Information S1.
[a]US Department of Agriculture sediment texture categories.

& Trompille, 2009). Through its global use, the model has been calibrated, repeatedly validated, and revised as needed (the current version is 20.1). In this study, because accurate measurement data to calibrate or validate the model were not available, we rely on this global validation history and standardized parameter values to model indicative end-member scenarios and predict a range of possible compaction values at Myrtle Grove. Through this modeling exercise, we obtain first-order insights into the response of the Mississippi Delta subsurface to sediment diversion-related loading.

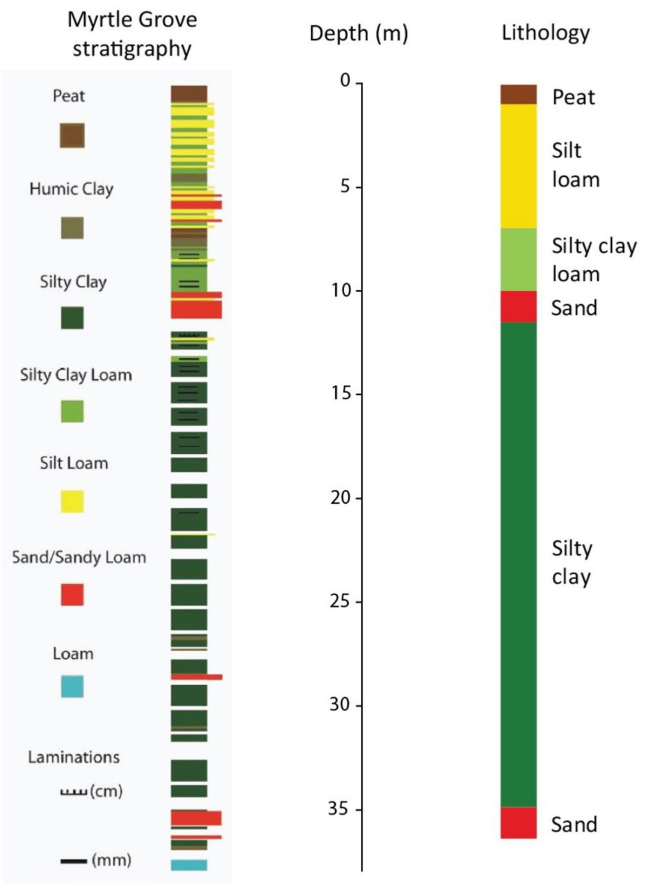

Figure 2. To streamline geotechnical modeling, the stratigraphy in the Myrtle Grove core (left, from Bridgeman (2018)) was simplified into six lithologic units (right).

D-Settlement is a two-dimensional model that incorporates processes of settlement (vertical lowering due to sediment compression and the resulting instantaneous volume change), primary consolidation (time-dependent volume reduction resulting from the release of over-pressurized porewater), and creep (secondary consolidation that continues after the sediment has reached a new pressure equilibrium). A detailed review of these processes is provided by Van Asselen et al. (2009). The D-Settlement modeling relies on the Darcy model of fluid flow through a porous medium and the Netherlands Standardization Institute (NEN) Bjerrum model of settlement, which uses linear strain sediment parameters (listed in Table 1 and described below) and follows the international standard for large strain settlement predictions (Deltares, 2018; see alsoBjerrum, 1967; Den Haan, 1994; Van der Meijs, 2015). The two primary limitations of the model are that, first, no horizontal deformation is included, and second, the geometry is not updated during the calculations. Neither of these limitations hinder the use of D-Settlement in this study. Further limitations and assumptions underlying the D-Settlement model and the NEN Bjerrum rheology are discussed in Deltares (2018).

The Myrtle Grove core was selected for modeling because it is nearly 40 m in length and contains relevant features such as peat intervals as well as sandier layers. It serves as a typical example of thick, deltaic strata and is reasonably representative of the lower Mississippi Delta. Both the thickness of the Holocene sediment package (~40 m) and the deltaic succession at Myrtle Grove are broadly similar to conditions in larger parts of the delta (Fisk & McFarlan, 1955; Stanley et al., 1996).

In order to streamline the modeling, the stratigraphy from the Myrtle Grove core (Bridgeman, 2018) was simplified into six lithologic units (Figure 2; Table 1). Each lithology was given fixed values for the unit weights above and below the phreatic surface, vertical permeability, and over-consolidation ratio (OCR). OCR is a dimensionless parameter defined as the preconsolidation stress divided by the present effective stress (Deltares, 2018). The results of a set of preliminary model experiments indicated that smaller OCR

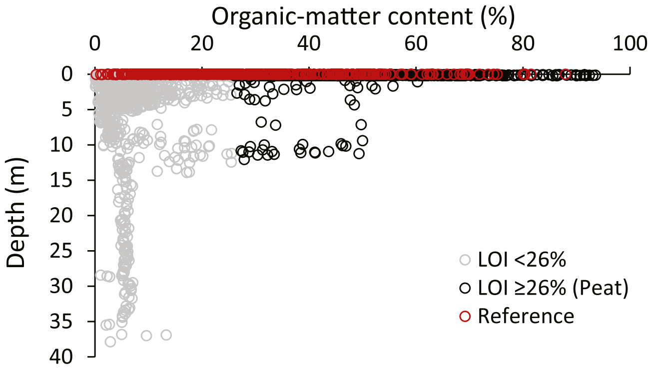

Figure 3. Organic-matter content versus depth for 2,865 sample intervals used in this analysis, including reference samples from the top 4 cm (red markers), peat samples at depths >4 cm (black markers, found only to depths <15 m), and samples with loss-on-ignition <26% at depths >4 cm (gray markers).

values lead to greater autocompaction (i.e., compaction that occurs without loading). For each sediment type, an OCR value between 1.00 and 2.00 was selected to reflect the role of autocompaction (an OCR of 2.00 produces no autocompaction in peat).

While OCR values were fixed, three related geotechnical parameters were allowed to vary. To bracket a range of likely outcomes, two endmember stratigraphies ("weak stratigraphy" and "stiff stratigraphy") were modeled for each lithology, using the typical ranges (see Table S3 in Supporting Information S1; Kooi et al., 2018; Netherlands Standardization Institute (NEN), 2006) for the reloading or swelling ratio (RR), compression ratio (CR), and the coefficient of secondary compression (Cα; Table 1). RR is used to calculate the elastic component of settlement that occurs at stresses less than the pre-loading stress. It relates the linear strain to the logarithm of stress during unloading. CR and Cα are used to calculate the settlement that occurs at stresses greater than the pre-loading stress. CR relates the linear strain to the logarithm of the stress during initial loading. Cα is used to calculate the secondary, time-dependent settlement. It relates linear strain to the logarithm of time after initial loading. Note that these three parameters are dimensionless ratios. Complete mathematical definitions are given in the D-Settlement User Manual (Deltares, 2018).

The two stratigraphies ("weak" and "stiff") were each subjected to three different loads (no loading, intermediate loading, high loading) for a total of six scenarios. For the intermediate and high loading scenarios, the load consisted of silty clay loam (with a unit weight of 20 kN m^{-3} above and 19 kN m^{-3} below the phreatic surface) deposited at a rate of 1 and 5 cm yr^{-1}, respectively, for 50 years. These accretion rates are comparable to rates observed seasonally in portions of the Mississippi Delta that are actively receiving river sediments (e.g., Keogh et al., 2019; Rosenheim et al., 2013), and that can persist for up to centuries (Shen et al., 2015). The yearly load was deposited instantaneously on the first day of each model year. In the no-loading scenarios, an extremely small load of very low-density material was required in order to allow the model to run (a 1 mm-thick deposit with a unit weight of 10 kN m^{-3} above and below the phreatic surface). The phreatic surface was set at 1 mm below the land surface for each scenario (a phreatic surface below the ground surface was required in order for the model to run). Accretion of load material was assumed to occur above the phreatic surface. The model was allowed to run for 100 years with results available at daily time steps.

4. Results

4.1. Organic-Matter Content—Bulk Density Relationship

The 330 sediment cores used for this analysis include a total of 2,865 sample intervals with paired bulk density and LOI measurements. Of the 2,436 sample intervals at depths >4 cm, 815 have LOI ≥26% (defined here as peat) and 1,621 have LOI <26% (Figure 3). Bulk density of samples in the reference data set ranges from 0.02 to 1.81 g cm^{-3} with a mean of 0.35 g cm^{-3}.

For our reference data set of uncompacted sediments, we find that the best-fit relationship between OM content (LOI) and bulk density (ρd_u) takes the form,

$$\rho d_u = a / \left(1 + a \times b \times \text{LOI}\right) \tag{7}$$

where $a = 2.296$ and $b = 0.139$ ($r^2 = 0.84$; Figure 4). Although this best-fit equation falls slightly below the equations used in Van Asselen (2011) and Morris et al. (2016), the curves are similar in shape. Unlike the equation used in Van Asselen (2011), which was fit to fall just below their reference data cloud of uncompacted peat, our equation was fit to the center of our reference data cloud. We conclude that surface sediments in coastal Louisiana are less anthropogenically impacted and thus more likely to be entirely uncompacted than those found in the Rhine-Meuse Delta, which has been extensively modified by humans over the past 1,000 years (Erkens

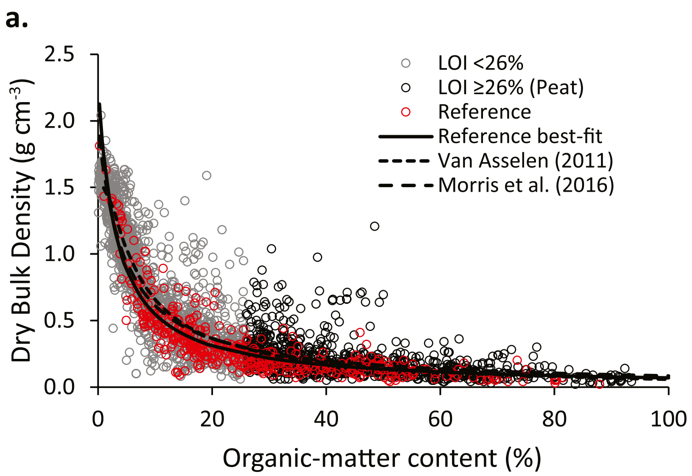

Figure 4. Relationship between organic matter (OM) content and bulk density for all 2,865 sample intervals, sorted by OM content (a) and data source (b): Coastwide Reference Monitoring System ($n = 1{,}584$), West Bay ($n = 788$), Myrtle Grove ($n = 137$), Davis Pond ($n = 194$), and Upper Lafourche ($n = 162$). The solid line in both panels represents the best-fit equation that is used for subsequent analyses ($r^2 = 0.84$). In panel (a), the dotted line and the dashed line represent the best-fit equations used in Van Asselen (2011) and Morris et al. (2016), respectively.

et al., 2016). The Morris et al. (2016) equation fits to the center of their data cloud, which consists of sediment samples from United States coastal marshes collected primarily in the uppermost 0.5 m (thus including both potentially compacted and uncompacted sediments).

Note that because our best-fit line plots through the center of the reference data cloud, some of the data points fall below the line (Figure 4). We have chosen to include these samples in our data set because they represent cases where our methods under-predict compaction and balance out instances where our method may over-predict compaction.

4.2. Impact of Burial Depth and Effective Stress on Sediment Compaction

We find a tight relationship between burial depth and effective stress (Figure 5). In general, sediment compaction increases with burial depth and thus effective stress (Figure 6). However, the shape of the compaction ratio versus depth curve depends on OM content. For sediments with LOI ≥5% (i.e., excluding only the most MM-dominated sediments; Figure 6a), the average compaction ratio changes approximately linearly with depth. When the analysis is limited to samples with greater OM content, the compaction ratio versus depth relationship becomes increasingly logarithmic (Figures 6b and 6c). After initially rapid decreases in compaction ratio with depth, compaction proceeds at a much slower pace at depths >3 m.

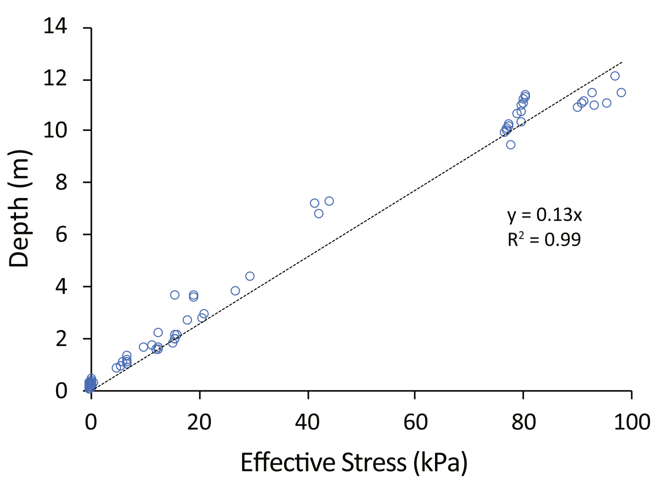

Figure 5. Effective stress versus depth for 815 organic-rich sediment and peat samples at depths ≥4 cm.

Typically, sediment with higher OM content is more compacted than less organic sediment under the same effective stress. At depths of 2–5 m, the average compaction ratio increases from ~60% in peat (LOI ≥26%, Figure 6c) to ~85% for sediments with LOI >5%, Figure 6a). Notably, however, a significant amount of compaction has occurred in sediments with a mineral-supported matrix (Figure 6a), particularly at greater depths. In the Myrtle Grove core, for example, a thick interval of MM-dominated silty clay (~11.5–35 m depth) has a mean compaction ratio of 79 ± 8%.

Age also appears to have an impact on compaction rate (Figure 7). In sediment with LOI ≥5%, the average compaction rate decreases rapidly from ~3 mm yr^{-1} m^{-1} in the 0–10 years age bin to ~2 mm yr^{-1} m^{-1} in the 30–100 years age bin (Figure 7a). This initial drop in compaction rate is even more pronounced in peat, which initially compacts at rates as high as ~5 mm yr^{-1} m^{-1} (Figure 7c). In bulk sediment ≥100 years old, the compaction rate

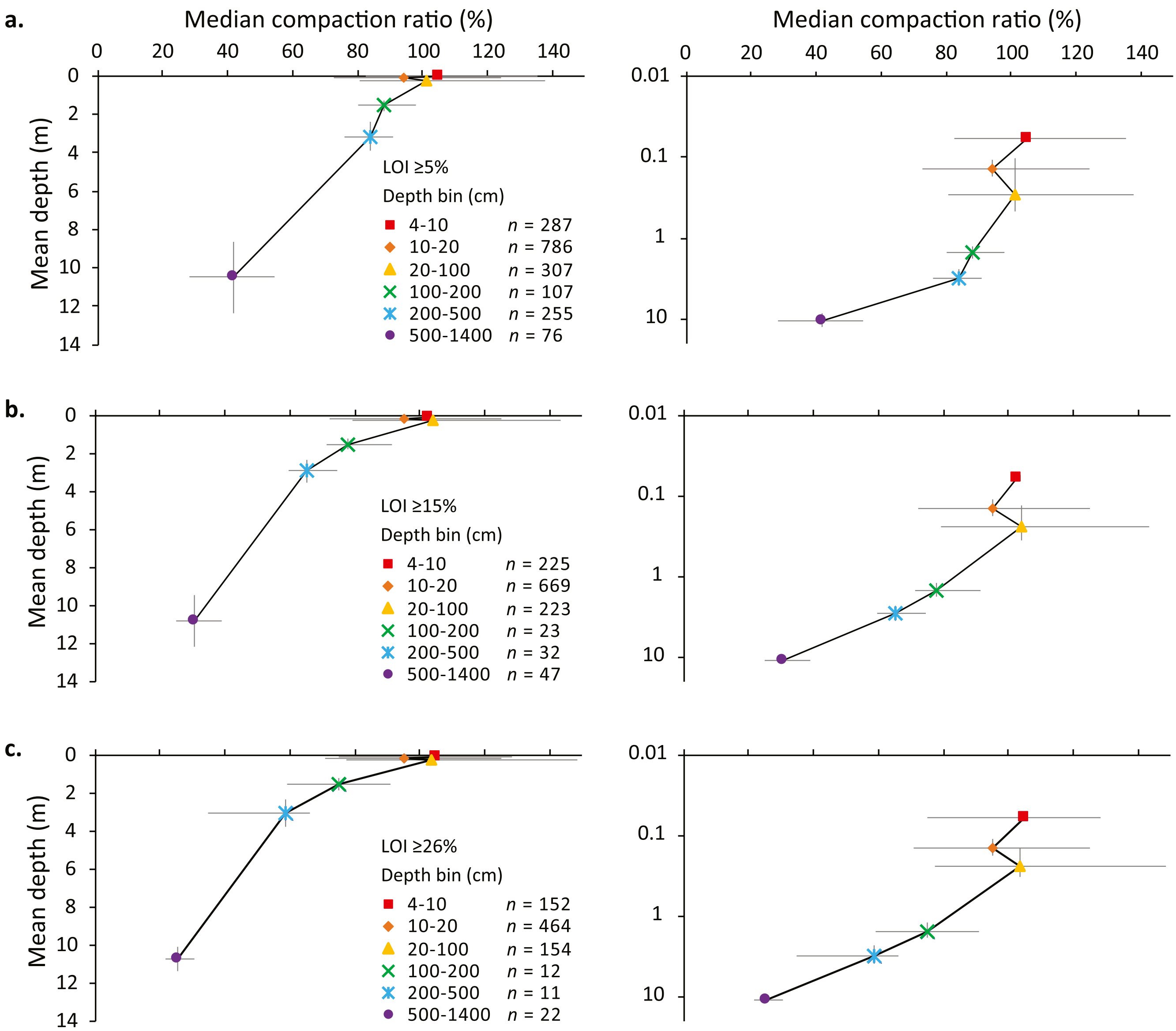

Figure 6. Median compaction ratio versus mean depth for samples in six depth bins. A compaction ratio of 100% means that the sample is 100% of its original thickness (i.e., uncompacted). Horizontal error bars span the 25th to 75th percentile of each bin. Vertical error bars represent one standard deviation around the mean sample depth. The OM content limit increases from 5% (a), to 15% (b), to 26% (c). In each panel, samples with OM contents below this limit are excluded. Note that the data shown in panel (c; $n = 815$) are a subset of the data in panel (b; $n = 1,219$), which are in turn a subset of those in panel (a; $n = 1,818$). Depth is plotted on a linear scale in the left-hand panels and on a log scale in the right-hand panels. Myrtle Grove data are excluded here because this core is almost 40 m deep and would produce a very wide depth range for the oldest age bin.

decreases to <1 mm yr^{-1} m^{-1} (Figure 7a) whereas the compaction rate in older peat samples is more variable (Figure 7c). This variability likely stems from shallow root expansion, which is common in organic-rich sediments and peat (e.g., Nyman et al., 1990), and is further reflected by the large horizontal error bars seen in Figures 6 and 7. Regardless of OM content, compaction rates have decreased by ~50% or more in ≥100-year-old samples, suggesting that most compaction occurs within the first 100–500 years after deposition and in the top 1–3 m of the subsurface (Figures 6 and 7).

For cores longer than 50 cm, the compaction in each sample interval was integrated to calculate the total thickness loss that has occurred due to compaction. Because sediment accretion and compaction occur simultaneously, the thickness loss values presented here do not represent true elevation loss. The total compaction ratio, which depends heavily on core length and local stratigraphy, ranges from 50% to 96% (i.e., sediments are 50%–96%

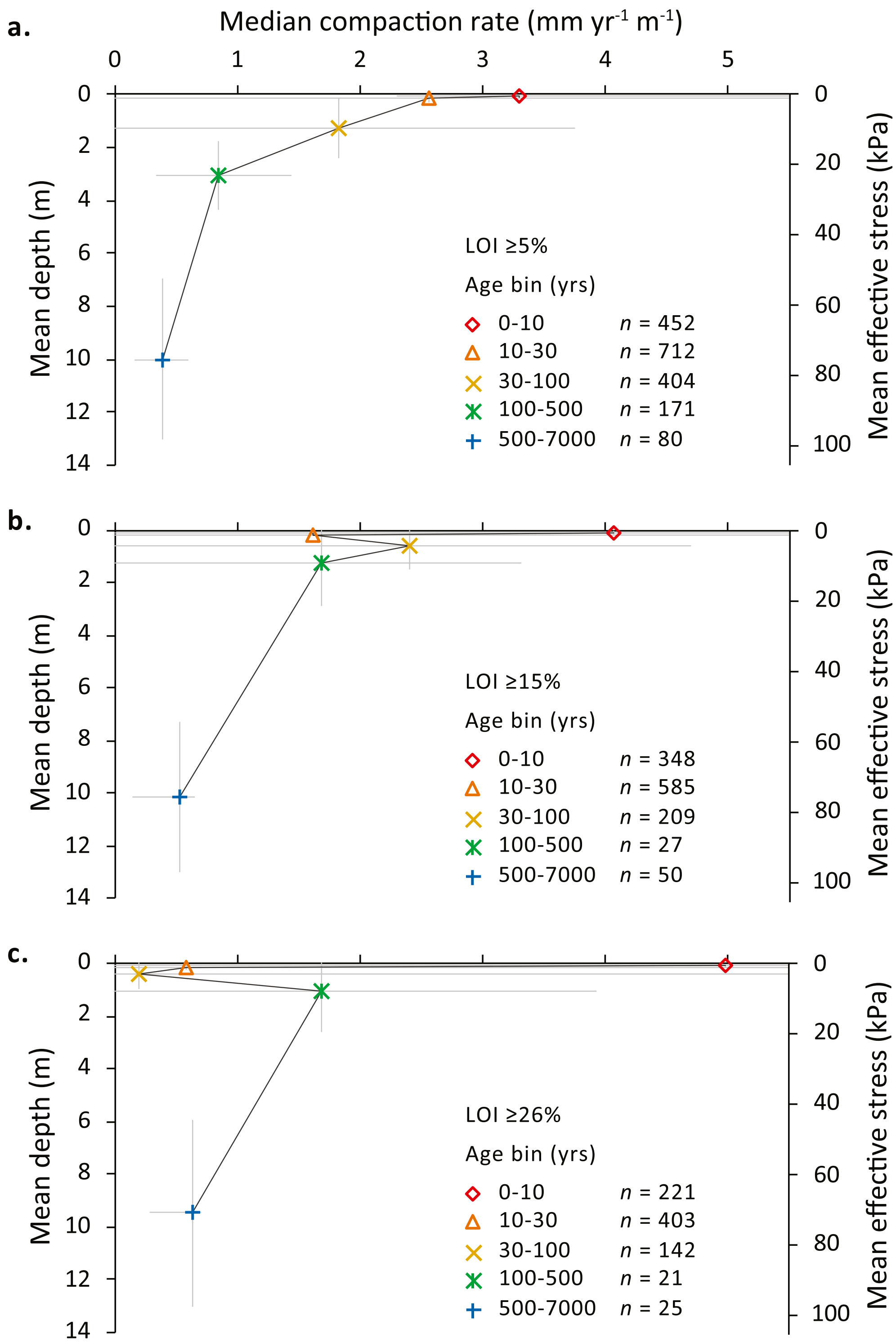

Figure 7. Median compaction rate versus mean depth per sample interval for five age bins. Horizontal error bars span the 25th to 75th percentile of each bin. Vertical error bars represent one standard deviation around the mean sample depth. For clarity, the full extent of some horizontal error bars is not shown. In each panel, samples with OM contents below the limit are excluded. Note that the data shown in panel c (n = 812) are a subset of the data in panel b (n = 1,219), which are in turn a subset of those in panel a (n = 1,819). As in Figure 6, Myrtle Grove data are excluded.

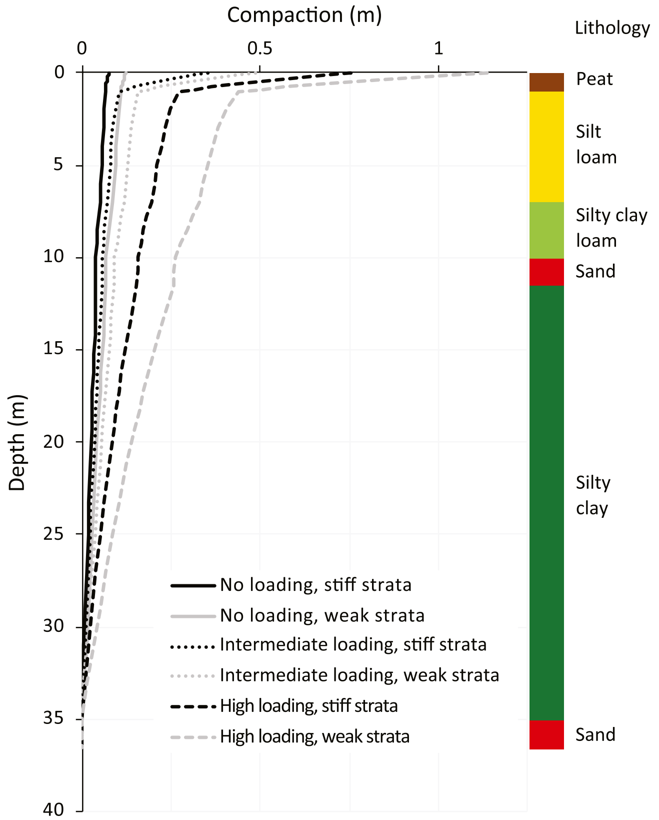

Figure 8. Six model scenarios showing potential compaction of the Myrtle Grove stratigraphy.

of their original thickness). The Myrtle Grove core that contains the entire Holocene sediment package exhibits a total compaction ratio of 82%, which corresponds to a thickness loss of 8.3 m over ∼11,500 years and is comparable to the compaction calculated by Zoccarato et al. (2020). The total compaction ratio in the three Upper Lafourche cores ranged from 50% to 62%, corresponding to thickness losses of 7.4–11.9 m over ∼1,000–7,000 years. In West Bay, where younger sediments were sampled in shorter cores, the top 3–5 m of strata have experienced less extensive compaction (mean $C_{\mathrm{ratio}} = 89 \pm 5\%$), which corresponds to a thickness loss of 0.5 ± 0.3 m over 170 ± 70 years. In Davis Pond, the 0.5-m core, which is comprised of very young sediments, has a total compaction ratio of 92%, resulting in a thickness loss of 0.04 m over ∼5 years.

4.3. Potential for Future Compaction

Although in the Mississippi Delta the Holocene sediment package has already compacted to as little as half its original thickness, modeling using D-Settlement suggests that some additional compaction is possible if the wetlands are loaded by renewed sediment deposition. At the Myrtle Grove site, the four model scenarios that simulated intermediate and high loading resulted in 0.35–1.14 m of compaction ($C_{\mathrm{ratio}} = 96.9\%–99.0\%$; Figure 8). Unlike the theoretical thickness losses reported above (Section 4.2), this is an estimate of true thickness loss. For comparison, the two no-loading scenarios produce very minor compaction ($C_{\mathrm{ratio}} = 99.7\%–99.8\%$). Much of the compaction occurs in the peat layer at the top of the sediment column. Although this peat layer is only 1 m thick, it compacts to 25%–70% of its original thickness, depending on the loading scenario, and contributes 62%–71% of the total compaction. The 23.5-m thick layer of silty clay also contributes significantly to the total compaction. Although the silty clay compacts to a C_{ratio} of only 97.0%–99.9% in the loading scenarios, it contributes 16%–23% of the total compaction due to its thickness. Detailed results from all six model scenarios are given in Table 2.

5. Discussion

Compaction-driven subsidence is both large in magnitude and widespread across deltas globally (e.g., Allison et al., 2016; Bijlsma et al., 1996; Higgins, 2016; Jankowski et al., 2017; Marriner et al., 2012; Mazzotti et al., 2009; Milliman & Haq, 1996; Shirzaei et al., 2021; Syvitski et al., 2009; Teatini et al., 2011; Törnqvist et al., 2008; Van Asselen, 2011; Zhang et al., 2015). Although compaction-driven subsidence is an integral part of the delta cycle (e.g., Coleman, 1988), unabated compaction that is not offset by deposition threatens the stability of current deltaic ecosystems and infrastructure.

5.1. The Role of Overburden in Driving Peat Compaction

In the Mississippi Delta, where MM- and OM-dominated strata are commonly interbedded in thick packages, sediment compaction is generally the predominant contributor to subsidence (e.g., Meckel et al., 2006; Jankowski et al., 2017; Penland & Ramsey, 1990; Törnqvist et al., 2008). The compaction ratio for peat (measured by length) in the top ∼10 m appears to reach a minimum at ∼25% (Figure 6). Below ∼3 m depth (∼20 kPa and up to the maximum observed effective stresses of ∼100 kPa), increases in overburden loading cause slower increases in compaction of peat (LOI ≥26%). Compaction continues to occur below this depth, albeit at a slower pace. Under deep burial and a full peat-to-coal transition, the compaction ratio can attain values of ∼10% (e.g., Nadon, 1998). In the Mississippi Delta, most peat compaction occurs rapidly after burial, and we find that about half of the observed compaction has occurred by the time sediment samples reach depths of ∼3 m (∼20 kPa, Figure 5). A closer analysis of changes in compaction rate with depth and age suggests that most compaction occurs in the top

Table 2
D-Settlement Model Results of Six Scenarios Showing Potential Compaction of Stratigraphy at the Myrtle Grove Site

Modeling scenario	Lithology	Original thickness (m)	Compacted thickness (m)	Total compaction (m)	Compaction ratio (% of layer)	Compaction (% of total)	Total accretion (load thickness; m)	Net surface elevation change (m)
No loading, weak strata	Peat	1	0.99	0.12	1.30	10.66	0.001	−0.12
	Silt loam	6	5.98		0.38	18.85		
	Silty clay loam	3	2.98		0.60	14.75		
	Sand (upper)	1.5	1.50		0	0		
	Silty clay	23.5	23.43		0.29	55.74		
	Sand (lower)	1.5	1.50		0	0		
No loading, stiff strata	Peat	1	0.99	0.07	0.90	12.16	0.001	−0.07
	Silt loam	6	5.99		0.25	20.27		
	Silty clay loam	3	2.99		0.33	13.51		
	Sand (upper)	1.5	1.5		0	0		
	Silty clay	23.5	23.46		0.17	54.05		
	Sand (lower)	1.5	1.5		0	0		
Intermediate loading, weak strata	Peat	1	0.67	0.49	33.10	67.69	0.5	0.01
	Silt loam	6	5.96		0.68	8.38		
	Silty clay loam	3	2.97		0.87	5.32		
	Sand (upper)	1.5	1.5		0.00	0.00		
	Silty clay	23.5	23.41		0.39	18.61		
	Sand (lower)	1.5	1.5		0	0		
Intermediate loading, stiff strata	Peat	1	0.75	0.35	24.80	70.66	0.5	0.15
	Silt loam	6	5.97		0.53	9.12		
	Silty clay loam	3	2.99		0.47	3.99		
	Sand (upper)	1.5	1.5		0.00	0.00		
	Silty clay	23.5	23.44		0.24	16.24		
	Sand (lower)	1.5	1.5		0	0		
High loading, weak strata	Peat	1	0.3	1.14	70.00	61.57	2.5	1.36
	Silt loam	6	5.89		1.80	9.50		
	Silty clay loam	3	2.93		2.23	5.89		
	Sand (upper)	1.5	1.50		0.20	0.26		
	Silty clay	23.5	23.24		1.10	22.69		
	Sand (lower)	1.5	1.50		0.07	0.09		
High loading, stiff strata	Peat	1	0.52	0.75	48.00	63.75	2.5	1.75
	Silt loam	6	5.92		1.30	10.36		
	Silty clay loam	3	2.96		1.33	5.31		
	Sand (upper)	1.5	1.50		0.07	0.13		
	Silty clay	23.5	23.35		0.66	20.45		
	Sand (lower)	1.5	1.5		0	0		

1–3 m below the land surface and within the first 100–500 years after deposition (Figures 6 and 7). Below this depth, the rate of sediment compaction decreases rapidly to <50% of the rate seen in the shallowest subsurface on a similar timescale as suggested by previous studies (e.g., Van Asselen et al., 2011; Zoccarato & Da Lio, 2021; Zoccarato & Teatini, 2017). As a result, subsidence measurements that are based on methods that do not capture

Table 3
Compaction Ratios and Corresponding Effective Stresses (Where Available) and Depths for a Variety of Coastal/Deltaic Wetlands Around the World

Location	Dominant sediment type	Minimum observed compaction ratio	Effective stress	Depth	Maximum vertical displacement	References
Deltaic wetlands						
Upper Lafourche, Mississippi Delta, Louisiana, USA	Mud-dominated overbank deposits and peat	25%	85 kPa	11 m	7 m	This study; Törnqvist et al. (2008)
Mekong Delta, Vietnam	Clay, commonly organic	30%	53 kPa	18 m	8.5 m	Zoccarato et al. (2018)
Rhine-Meuse Delta, the Netherlands	Anthropogenic clay and loam	35%	70 kPa	9 m	N/A	Van Asselen et al. (2018)
Rhine-Meuse Delta, the Netherlands	Peat	45%	25 kPa	5 m	3 m	Van Asselen (2011) and Van Asselen et al. (2018)
Non-deltaic coastal wetlands						
Singapore	Marine clay	33%	N/A	9 m	0.28 m	Bird et al. (2004)
Coastal Connecticut, USA	Sedge peat	44%	N/A	3.3–10.9 m	~2 m	Bloom (1964)
Bristol Channel, UK (18 km inland)	Peat overlain by intertidal clay	45%	N/A	~2 m	N/A	Haslett et al. (1998)
Tump Point, North Carolina, USA	Saltmarsh peat	88%	<3 kPa	~1.6 m	0.023 m	Brain et al. (2015)
Big River Estuary, Newfoundland, Canada	Saltmarsh peat	99%	~3 kPa	3.2 m	<0.02 m	Kemp et al. (2018)
Inland wetlands						
Cumberland Marshes, Saskatchewan, Canada	Peat	60%	N/A	~10 m	N/A	Van Asselen et al. (2011)

the top 1–3 m (e.g., global navigation satellite systems; GNSS) are likely to record an incomplete subsidence signal and thus underestimate the subsidence rate (Keogh & Törnqvist, 2019).

Observed maximum compaction ratios vary between deltas (Table 3), perhaps driven by local differences in loading, thickness of Holocene sediment, OM content, and drainage, and affected by processes of peat degradation due to oxidation and diagenetic remineralization. Due to the relatively thin and peat-dominated Holocene sediment package in the Rhine-Meuse Delta (up to 20–25 m; Pons et al., 1963), natural loading produces effective stresses of generally no more than ~25 kPa (Van Asselen et al., 2018). In comparison, Mississippi Delta sediments may be up to four times thicker (50–100 m; Kolb & Van Lopik, 1966) and possess less OM. Observed effective stresses in the Mississippi Delta are up to 100 kPa, which corresponds to ~13 m depth (Table S1, Figure 5). At the mouth of the Mississippi River, the Holocene sediment package is >100 m thick and could potentially produce effective stresses of >750 kPa if the approximately linear depth-effective stress relationship persists. Anthropogenic loading (e.g., embankments) in the Rhine-Meuse Delta can produce effective stresses up to 60–70 kPa, and hypothetical further increases in effective stress (e.g., due to artificial drainage) may lead to greater compaction, possibly approaching values observed at similar depths in the Mississippi Delta.

Studies of wetlands in coastal Louisiana consistently find that sediment compaction is the primary driver of subsidence (e.g., Cahoon et al., 1995; Jankowski et al., 2017; Törnqvist et al., 2008). Compaction rates along the U.S. Atlantic Coast are commonly lower, however, probably due to the fact that marshes in this region are typically highly organic (≥30% LOI; Bricker-Urso et al., 1989; Kolker et al., 2009; Redfield, 1972) and thus have effective stresses that may be too low to drive autocompaction (Brain et al., 2015, Table 3).

Some peats may reach lower compaction ratios because they start out at a lower bulk density. The close coincidence of the Morris et al. (2016) best-fit curve (which represents a combination of compacted and uncompacted sediments) and the Van Asselen (2011) curve (which is intended to represent uncompacted sediments only) together with the observation that our best-fit equation for uncompacted sediments plots below both of these curves, suggests that the reference datasets used in these other studies may not have been entirely compaction-free. Reference samples used in both Van Asselen (2011) and Morris et al. (2016) were primarily from the top 70 cm but were not confined to the uppermost 4 cm as in our study. Furthermore, even in the top 4 cm, peat in the Rhine-Meuse Delta will have a higher bulk density than Mississippi Delta peats because water management (i.e., groundwater level lowering) in The Netherlands leads to compaction even without loading (e.g., Erkens et al., 2016; Van Asselen et al., 2018).

5.2. The Future of Deltaic Wetlands

In the modern era of accelerated RSLR, increased sediment accretion will be essential for the survival of many deltas (Giosan et al., 2014). Although wetlands starved of regular sediment deposition tend to rapidly lose elevation, renewed sedimentation can dramatically increase vertical accretion rates over short timescales. In the Ganges-Brahmaputra Delta, for example, poldered islands have lost up to 1.5 m of elevation while neighboring un-embanked wetlands have remained stable (Auerbach et al., 2015). After catastrophic cyclone-related embankment failure occurred on one poldered island, the interior of the island was reconnected to tidal flooding and sediment accretion rates increased by an order of magnitude. Over two years, tens of cm of new sediment were deposited in the subsided interior of the island (Auerbach et al., 2015). Similarly high rates of vertical accretion have occurred in the Sacramento-San Joaquin Delta, where leveed islands have subsided by up to 7 m below sea level and intentional flooding resulted in sediment accumulation rates of up to 9 cm yr^{-1} (Miller et al., 2008). In the Mississippi Delta, sediment delivery to the mouth of the Atchafalaya River and through the Wax Lake Outlet resulted in rapid growth of new delta lobes, where 59 km^2 of new land emerged over a span of just 21 years (1989–2010; Rosen & Xu, 2013).

In the Mississippi Delta, river diversions represent one of the primary methods proposed to combat RSLR (CPRA, 2017; Day et al., 2007; Gagliano & Van Beek, 1975; Kolker et al., 2018; Paola et al., 2011; Peyronnin et al., 2017; Xu et al., 2019). Diversions are engineered outlet channels that divert a portion of the river's water, sediment, and nutrient load into an adjacent wetland in a controlled manner. In order for diversions to be successful in building land, the thickness of newly deposited sediment must exceed the elevation lost to compaction (Paola et al., 2011; Reed, 2002; Törnqvist et al., 2008). It is possible that renewed sediment deposition in peat-rich wetlands may cause more elevation loss to compaction than is gained due to accretion due to the increased loading from the new sediment. In extreme cases, sudden introduction of MM to a low-density, OM-dominated system could cause rapid wetland drowning and conversion to open water. On the other hand, wetlands overlying crevasse splays and other MM-dominated facies may support the weight of renewed deposition and allow for net elevation gain. Even with higher compaction rates, however, wetland building can be successful. Modeling by Nienhuis et al. (2018) found that the largest crevasse splays form in association with moderate sediment compaction, which provides the accommodation necessary for the accumulation of new material and prevents choking of the feeder channel. Time is an important consideration, however: land built by an initially successful crevasse splay will continue to subside as a result of slower but continuous compaction, which may counteract land gain unless sediment input is sustained.

The model results presented here suggest that the stratigraphy at Myrtle Grove may successfully support the weight of diversion-deposited sediments. Although renewed deposition from a river diversion may cause as much as 1.14 m of compaction, vertical accretion is predicted to outpace compaction and result in a net elevation gain of 0.01–1.75 m in 100 years, depending on the size of the diversion and the stiffness of the underlying sediment (Table 2). Higher sediment loading causes more compaction, but also increases net surface elevation gain. Conversely, moderate sediment loading produces less compaction and less surface elevation gain. Surface elevation gain is maximized with high sediment loading and stiff strata.

Multiple new river diversions are currently planned for the lower Mississippi Delta, and their success will be critical for wetland restoration efforts (CPRA, 2017). Because sediment deposition rate can be considered a proxy for diversion size (i.e., water discharge capacity), our model results suggest that a larger river diversion will be more successful in terms of net elevation gain than a smaller diversion in a given location. Net elevation gain is as much as 13.5 times greater when the pre-existing strata are stiffer and compaction is limited (Table 2). Stiffer stratigraphy becomes increasingly important with larger diversions that deposit more sediment. As a result, river diversions must be sited thoughtfully. The results presented here suggest that Myrtle Grove, nearby the proposed Mid-Barataria Sediment Diversion, is a potentially suitable location for a diversion in terms of compaction, although further geotechnical analysis could reduce uncertainties. The results of this study encourage the future use of geotechnical modeling, including experimentation with different subsurface architecture and diversion loading scenarios, to support river diversion site investigation. In such detailed studies, it will be important that the model input parameters are derived from local measurements and land subsidence time series data must be available for model calibration and validation.

Although river diversions may be viable tools for coastal restoration at MM-dominated locations such as Myrtle Grove, other portions of the Mississippi Delta are much more organic, as may be the case in other deltas. The Rhine-Meuse Delta, for example, contains extensive peat beds (Van Asselen et al., 2018). In this type of environment, deposition of dense, mineral sediment from a river diversion may cause more compaction of the peat than is made up for with vertical accretion, rendering the diversion counterproductive. Interestingly, some deltas such as the Mekong have exceedingly high rates of sediment compaction despite being MM-dominated (Zoccarato et al., 2018). The rapidly compacting Mekong Delta sediments are relatively young (<3,000 years) and were deposited in a comparable setting as the modern mouth of the Mississippi River. In the Mississippi Delta, we find that MM-dominated sediments commonly have compaction ratios of ∼50% and can have ratios as low as 20% (Table S1). Although it is possible that additional loading in the Rhine-Meuse Delta could decrease the compaction ratio to below what we observe in the Mississippi Delta (due to the current low MM content and lack of loading of the Rhine-Meuse sediments), surface elevation loss due to loading would likely be greater in the Mississippi Delta because of its much larger thickness of Holocene strata.

Some previous studies have suggested that OM accretion alone may be sufficient for coastal wetlands to keep pace with RSLR (e.g., Turner, 1997). This may be true in specific locations where intact wetlands are dominated by peat growth and experience no mineral input. In such circumstances, which are rare in deltaic wetlands, peat loading and compaction are both minimal. However, given that OM-rich strata can exhibit compaction ratios as low as 25% when loaded with MM, our findings show that deltas are unlikely to simply grow themselves out of their elevation deficit even if short-term vertical accretion rates equal or exceed rates of RSLR. Instead, even with abundant OM the import of mineral sediment is critical to wetland accretion (Mariotti et al., 2020). If sediment delivery to a deteriorating, organic-rich wetland is substantially increased via a river diversion, net elevation loss may be reversed (e.g., Keogh et al., 2019).

5.3. Implications for Sea-Level Reconstruction

Predicting delta sustainability benefits greatly from an understanding of past deltaic responses to changes in RSLR. Specifically, this requires reconstructions of RSLR for which deltaic strata offer excellent potential (e.g., Jelgersma, 1961; Tamura et al., 2009; Törnqvist et al., 2020; Van de Plassche, 1982). However, sediment compaction is a major obstacle to high-resolution reconstruction of past rates of RSLR. Ideally, compaction-free sea-level indicators are used for these purposes, but this is not always feasible. Thus, corrections for sediment compaction are needed. This could involve geotechnical modeling (Brain, 2015; Walker et al., 2021) such as the D-Settlement model used herein; however, this requires detailed information on sediment properties that is not always available. Therefore, recourse has been taken to carrying out simpler corrections. Even for samples resting on largely compaction-free substrates (e.g., basal peats) a correction is needed for the fact that the sampled interval (i.e., the peat layer itself) has lost thickness compared to its original state. A correction factor of 2.5 has been used to account for this (Hijma et al., 2015; Van de Plassche et al., 2005), in part based on the work by Van Asselen (2011). Our new findings show that such a value (equivalent to a compaction ratio of 40%) is commonly attained within 10 m of burial. Even much shallower samples from settings comparable to ours are likely to have seen substantial compaction within the first few meters, something that is often ignored in the sea-level literature. We find that sediments with effective stresses as low as ∼10 kPa are likely to have experienced substantial compaction. For more deeply buried or heavily loaded samples, compaction correction factors of up to 4 (corresponding to a compaction ratio of 25%, the lowest value we observe in our data set) may be appropriate.

As mentioned earlier, conditions can be quite different in highly organic marshes that have experienced minimal artificial drainage. For example, recent sea-level studies from salt marshes along the Atlantic Coast of North America have shown that successions up to 3 m in thickness may have experienced very little compaction (Table 3). These are environments with highly organic strata (OM contents commonly 40%–70%) and unaltered hydrology with high porewater pressure, resulting in effective stresses generally <3 kPa (e.g., Brain et al., 2015; Brain et al., 2017; Kemp et al., 2018). Under such conditions, corrections may be on the order of a few cm only and can largely be ignored. In some cases, these findings can be extended to mangrove peats where recent work based on computed tomography scanning has demonstrated a lack of compaction in successions as thick as 12 m (Toscano et al., 2018).

Compaction conditions change rapidly, however, in circumstances where mineral sediment is introduced to an environment previously dominated by OM (Toscano et al., 2018). We see this in our D-Settlement modeling as well: the 1 m of peat at the surface in the Myrtle Grove core experiences essentially zero compaction under no-loading scenarios but reaches compaction ratios as low as 30% when MM is reintroduced. In environments that feature intercalated organic and mineral strata, displacements can be as high as 8 m (e.g., Bridgeman, 2018; De Groot & De Gans, 1996; Törnqvist et al., 2008). Such circumstances are important to recognize (and avoid) in paleo-RSLR reconstruction.

6. Conclusions

We present the first analysis of sediment compaction in deltaic deposits as a function of depth and time that covers timescales spanning four orders of magnitude (annual to millennial). This analysis is anchored by a large and globally unprecedented data set of undisturbed surface wetland sediments that have seen little if any compaction, and the complete data set has been made fully available for other researchers to use. We identify the depth range and timescale over which most sediment compaction occurs and make a first attempt at predictions regarding future compaction-driven surface-elevation change. We reach the following conclusions:

- A large proportion of the total observed sediment compaction of organic-rich (≥5% OM) strata in the Mississippi Delta occurs in the top 1–3 m, representing the first 100–500 years after deposition.
- Subsidence measurements in deltaic sediments that are based on methods that do not capture this depth range (e.g., GNSS) are likely to record an incomplete subsidence signal.
- Coastal successions with effective stresses of ∼10 kPa or more are likely to have experienced substantial compaction. This must be considered in stratigraphic studies of RSLR, unless sea-level indicators rest immediately on a compaction-free basement. Our data may offer new prospects for the correction of compaction-prone geological sea-level data for vertical displacement.
- For a given effective stress, compaction increases with an increasing OM content, with compaction ratios as low as ∼25% for peats buried at about 10 m depth (i.e., the measured thickness is about one quarter of the original deposit thickness). Therefore, OM accretion alone likely cannot sustain a deltaic plain facing accelerated RSLR because such deposits will ultimately succumb to high compaction rates.
- In the Mississippi Delta, the Holocene sediment package has already lost 10%–50% of its potential thickness due to compaction. Modeling of future compaction for a nearly 40-m-thick deltaic succession that spans the entire Holocene and that has already lost ∼18% of its original thickness shows that an additional loss due to compaction from loading of up to 3% may occur in the next 100 years.
- Renewed MM deposition in deltaic wetlands causes substantial sediment compaction, especially over OM-dominated substrates. Nevertheless, planned river diversions in the Mississippi Delta are expected to produce net elevation gain, with the magnitude of gain (up to 1.75 m in 100 years) increasing with greater accretion rate (5 cm yr^{-1}) and stiffness of underlying strata.

Conflict of Interest

The authors declare no conflicts of interest relevant to this study.

Data Availability Statement

All supporting data are included in the Supporting Information section and are publicly accessible through the Dataverse data repository, available at: https://doi.org/10.7910/DVN/KOCAII. Coastwide Reference Monitoring System data are available online through the Coastal Protection and Restoration Authority's Coastal Information Management System at http://cims.coastal.louisiana.gov.

Acknowledgments

This research was funded by the US National Science Foundation (EAR-1349311) and the Coastal Science Assistantship Program of Louisiana Sea Grant. The authors would like to thank Krista Jankowski and Elena Steponaitis for providing data and field context, Sanneke van Asselen for support with the compaction calculations, and Henk Kooi for assistance with the D-Settlement model. Three anonymous referees enabled us to make improvements to the paper. This is a contribution to the PALSEA program and to IGCP Project 725 (Forecasting Coastal Change).

References

Abspoel, L., Courage, W., Dabekaussen, W., de Bruijn, R., Kruse, H., Wiersma, A. P., et al. (2018). Risk-based asset management: Automated structural reliability assessment of geographically distributed pipeline networks for gas and water in the Netherlands. *Structure and Infrastructure Engineering*, *14*, 928–940. https://doi.org/10.1080/15732479.2018.1437641

Adams, W. A. (1973). The effect of organic matter on the bulk and true densities of some uncultivated podzolic soils. *Journal of Soil Science*, *24*, 10–17. https://doi.org/10.1111/j.1365-2389.1973.tb00737.x

Allison, M., Yuill, B., Törnqvist, T., Amelung, F., Dixon, T. H., Erkens, G., et al. (2016). Global risks and research priorities for coastal subsidence. *Eos*, *97*(19), 22–27. https://doi.org/10.1029/2016eo055013

Auerbach, L. W., Goodbred, S. L., Jr., Mondal, D. R., Wilson, C. A., Ahmed, K. R., Roy, K., et al. (2015). Flood risk of natural and embanked landscapes on the Ganges–Brahmaputra tidal delta plain. *Nature Climate Change*, *5*, 153–157. https://doi.org/10.1038/nclimate2472

Baldwin, B. (1971). Ways of deciphering compacted sediments. *Journal of Sedimentary Petrology*, *41*, 293–301. https://doi.org/10.1306/74d7224d-2b21-11d7-8648000102c1865d

Bijlsma, L., Ehler, C. N., Klein, R. J. T., Kulshrestha, S. M., McLean, R. F., Mimura, N., et al. (1996). Coastal zones and small islands. In R. T. Watson, M. C. Zinyowera, & R. H. Moss (Eds.), *Climate change 1995. Impacts, adaptations and mitigation of climate change: Scientific-technical analyses* (pp. 289–324). Cambridge University Press.

Bird, M. I., Fifield, L. K., Chua, S., & Goh, B. (2004). Calculating sediment compaction for radiocarbon dating of intertidal sediments. *Radiocarbon*, *46*, 421–435. https://doi.org/10.1017/s0033822200039734

Bjerrum, L. (1967). Engineering geology of Norwegian normally consolidated marine clays as related to settlements of buildings. *Géotechnique*, *17*, 81–118. https://doi.org/10.1680/geot.1967.17.2.83

Bloom, A. L. (1964). Peat accumulation and compaction in a Connecticut coastal marsh. *Journal of Sedimentary Petrology*, *34*, 599–603. https://doi.org/10.1306/74d710f5-2b21-11d7-8648000102c1865d

Brain, M. J. (2015). Compaction. In I. Shennan, A. J. Long, & B. P. Horton (Eds.), *Handbook of sea-level research* (pp. 452–469). Wiley. https://doi.org/10.1002/9781118452547.ch30

Brain, M. J., Kemp, A. C., Hawkes, A. D., Engelhart, S. E., Vane, C. H., Cahill, N., et al. (2017). Exploring mechanisms of compaction in salt-marsh sediments using Common Era relative sea-level reconstructions. *Quaternary Science Reviews*, *167*, 96–111. https://doi.org/10.1016/j.quascirev.2017.04.027

Brain, M. J., Kemp, A. C., Horton, B. P., Culver, S. J., Parnell, A. C., & Cahill, N. (2015). Quantifying the contribution of sediment compaction to late Holocene salt-marsh sea-level reconstructions, North Carolina, USA. *Quaternary Research*, *83*, 41–51. https://doi.org/10.1016/j.yqres.2014.08.003

Brevik, E. C., & Homburg, J. A. (2004). A 5000 year record of carbon sequestration from a coastal lagoon and wetland complex, Southern California, USA. *Catena*, *57*, 221–232. https://doi.org/10.1016/j.catena.2003.12.001

Bricker-Urso, S., Nixon, S. W., Cochran, J. K., Hirschberg, D. J., & Hunt, C. (1989). Accretion rates and sediment accumulation in Rhode Island salt marshes. *Estuaries*, *12*, 300–317. https://doi.org/10.2307/1351908

Bridgeman, J. G. (2018). Understanding Mississippi Delta subsidence through stratigraphic and geotechnical analysis of a continuous Holocene core at a subsidence superstation (Master's thesis). Tulane University. Retrieved from Tulane University Digital Library https://digitallibrary.tulane.edu/theses_and_dissertations

Cahoon, D. R., Reed, D. J., & Day, J. W., Jr. (1995). Estimating shallow subsidence in microtidal salt marshes of the southeastern United States: Kaye and Barghoorn revisited. *Marine Geology*, *128*, 1–9. https://doi.org/10.1016/0025-3227(95)00087-f

Calvo-Cubero, J., Ibáñez, C., Rovira, A., Sharpe, P. J., & Reyes, E. (2013). Mineral versus organic contribution to vertical accretion and elevation change in restored marshes (Ebro Delta, Spain). *Ecological Engineering*, *61*, 12–22. https://doi.org/10.1016/j.ecoleng.2013.09.047

Chamberlain, E. L., Shen, Z., Kim, W., McKinley, S., Anderson, S., & Törnqvist, T. E. (2021). Does Load-Induced Shallow Subsidence Inhibit Delta Growth? *Journal of Geophysical Research: Earth Surface*, *126*(11). https://doi.org/10.1029/2021jf006153

Chant, R. J., Ralston, D. K., Ganju, N. K., Pianca, C., Simonson, A. E., & Cartwright, R. A. (2021). Sediment budget estimates for a highly impacted embayment with extensive wetland loss. *Estuaries and Coasts*, *44*, 608–626. https://doi.org/10.1007/s12237-020-00784-3

Coleman, J. M. (1988). Dynamic changes and processes in the Mississippi River delta. *Geological Society of America Bulletin*, *100*, 999–1015. https://doi.org/10.1130/0016-7606(1988)100<0999:dcapit>2.3.co;2

CPRA. (2017). *Louisiana's comprehensive master plan for a sustainable coast*. Coastal Protection and Restoration Authority of Louisiana.

CPRA. (2018). Coastwide Reference Monitoring System – Wetlands monitoring data. Coastal Information Management System (CIMS) database, Coastal Protection and Restoration Authority of Louisiana. Retrieved from http://cims.coastal.louisiana.gov

Day, J. W., Agboola, J., Chen, Z., D'Elia, C., Forbes, D. L., Giosan, L., et al. (2016). Approaches to defining deltaic sustainability in the 21st century. *Estuarine, Coastal and Shelf Science*, *183*, 275–291. https://doi.org/10.1016/j.ecss.2016.06.018

Day, J. W., Jr., Boesch, D. F., Clairain, E. J., Kemp, G. P., Laska, S. B., Mitsch, W. J., et al. (2007). Restoration of the Mississippi Delta: Lessons from Hurricanes Katrina and Rita. *Science*, *315*, 1679–1684. https://doi.org/10.1126/science.1137030

Day, J. W., Kemp, G. P., Reed, D. J., Cahoon, D. R., Boumans, R. M., Suhayda, J. M., & Gambrell, R. (2011). Vegetation death and rapid loss of surface elevation in two contrasting Mississippi Delta salt marshes: The role of sedimentation, autocompaction and sea-level rise. *Ecological Engineering*, *37*, 229–240. https://doi.org/10.1016/j.ecoleng.2010.11.021

De Groot, T. A. M., & De Gans, W. (1996). Facies variations and sea-level-rise response in the lowermost Rhine/Meuse area during the last 15000 years (the Netherlands). *Mededelingen Rijks Geologische Dienst*, *57*, 229–250.

DeLaune, R. D., Baumann, R. H., & Gosselink, J. G. (1983). Relationships among vertical accretion, coastal submergence, and erosion in a Louisiana Gulf Coast marsh. *Journal of Sedimentary Petrology*, *53*, 147–157. https://doi.org/10.1306/212f8175-2b24-11d7-8648000102c1865d

Deltares. (2018). *D-settlement embankment design and soil settlement prediction: User manual*. Deltares.

Den Haan, E. J. (1994). Vertical compression of soils (PhD dissertation). Technische Universiteit Delft. Retrieved from Technische Universiteit Delft Institutional Repository http://resolver.tudelft.nl/uuid:b8dc88e0-f400-4d86-9a2e-4e00b68d0472

Den Haan, E. J., & Kruse, G. A. M. (2007). Characterisation and engineering properties of Dutch peats. In T. S. Tan, K. K. Phoon, D. W. Hight, & S. Leroueil (Eds.), *Characterisation and engineering properties of natural soils, Proceedings of the second international workshop on characterisation and engineering properties of natural soils* (Vol. 3, pp. 2101–2134). Taylor and Francis.

Dunn, F. E., Darby, S. E., Nicholls, R. J., Cohen, S., Zarfl, C., & Fekete, B. M. (2019). Projections of declining fluvial sediment delivery to major Deltas worldwide in response to climate change and anthropogenic stress. *Environmental Research Letters*, *14*, 084034. https://doi.org/10.1088/1748-9326/ab304e

Edmonds, D. A. (2012). Restoration sedimentology. *Nature Geoscience*, *5*, 758–759. https://doi.org/10.1038/ngeo1620

Edmonds, D. A., Caldwell, R. L., Brondizio, E. S., & Siani, S. M. O. (2020). Coastal flooding will disproportionately impact people on river deltas. *Nature Communications*, *11*, 4741. https://doi.org/10.1038/s41467-020-18531-4

Erkens, G., van der Meulen, M. J., & Middelkoop, H. (2016). Double trouble: Subsidence and CO_2 respiration due to 1,000 years of Dutch coastal peatlands cultivation. *Hydrogeology Journal*, *24*, 551–568. https://doi.org/10.1007/s10040-016-1380-4

Esposito, C. R., Shen, Z., Törnqvist, T. E., Marshak, J., & White, C. (2017). Efficient retention of mud drives land building on the Mississippi Delta plain. *Earth Surface Dynamics*, *5*, 387–397. https://doi.org/10.5194/esurf-5-387-2017

Fisk, H. N., & McFarlan, E., Jr. (1955). Late Quaternary deltaic deposits of the Mississippi River. *Geological Society of America Special Paper*, *62*, 279–302.

Fisk, H. N., McFarlan, E., Jr., Kolb, C. R., & Wilbert, L. J., Jr. (1954). Sedimentary framework of the modern Mississippi Delta. *Journal of Sedimentary Petrology*, *24*, 76–99. https://doi.org/10.1306/d4269661-2b26-11d7-8648000102c1865d

Folse, T. M., Sharp, L. A., West, J. L., Hymel, M. K., Troutman, J. P., McGinnis, T. E., et al. (2012). *A standard operating procedures manual for the coast-wide reference monitoring system – Wetlands: Methods for site establishment, data collection, and quality assurance/quality control*. Louisiana Coastal Protection and Restoration Authority, Office of Coastal Protection and Restoration.

Fox-Kemper, B., Hewitt, H. T., Xiao, C., Aðalgeirsdóttir, G., Drijfhout, S. S., Edwards, T. L., et al. (2021). Ocean, cryosphere and sea level change. In V. Masson-Delmotte, P. Zhai, A. Pirani, S. L. Connors, C. Péan, S. Berger, et al. (Eds.), *Climate Change 2021: The Physical Science Basis. Contribution of Working Group I to the Sixth Assessment Report of the Intergovernmental Panel on Climate Change* (in press). Cambridge University Press.

Gagliano, S. M., & Van Beek, J. L. (1975). An approach to multiuse management in the Mississippi Delta system. In M. L. Broussard (Ed.), *Deltas: Models for exploration* (pp. 223–238). Houston Geological Society.

Giosan, L., Constantinescu, S., Filip, F., & Deng, B. (2013). Maintenance of large deltas through channelization: Nature vs. humans in the Danube delta. *Anthropocene*, *1*, 35–45. https://doi.org/10.1016/j.ancene.2013.09.001

Giosan, L., Syvitski, J., Constantinescu, S., & Day, J. (2014). Protect the world's deltas. *Nature*, *516*, 31–33. https://doi.org/10.1038/516031a

Haslett, S. K., Davies, P., Curr, R. H. F., Davies, C. F. C., Kennington, K., King, C. P., & Margetts, A. J. (1998). Evaluating late-Holocene relative sea-level change in the Somerset Levels, southwest Britain. *The Holocene*, *8*, 197–207. https://doi.org/10.1191/095968398669499299

Higgins, S. A. (2016). Advances in delta-subsidence research using satellite methods. *Hydrogeology Journal*, *24*, 587–600. https://doi.org/10.1007/s10040-015-1330-6

Hijma, M. P., Engelhart, S. E., Törnqvist, T. E., Horton, B. P., Hu, P., & Hill, D. F. (2015). A protocol for a geological sea-level database. In I. Shennan, A. J. Long, & B. P. Horton (Eds.), *Handbook of sea-level research* (pp. 536–553). Wiley. https://doi.org/10.1002/9781118452547.ch34

Hoefsloot, F. J. M. (2015). Evaluation Settlement Models Test Embankments Bloemendalerpolder – Geo-Impulse Program. In T. Schweckendiek, A. F.van Tol, D.Pereboom, M. Th.Pereboom, & P. M. C. B. M.Cools (Eds.), *Geotechnical safety and risk V* (pp. 628–633). IOS Press.

Hoitink, A. J. F., Nittrouer, J. A., Passalacqua, P., Shaw, J. B., Langendoen, E. J., Huismans, Y., & van Maren, D. S. (2020). Resilience of river deltas in the Anthropocene. *Journal of Geophysical Research: Earth Surface*, *125*, e2019JF005201. https://doi.org/10.1029/2019jf005201

Jankowski, K. L. (2018). Implications of environmental change on wetland vulnerability and carbon sequestration in coastal Louisiana (Doctoral dissertation). Tulane University Digital Library. Retrieved from https://digitallibrary.tulane.edu/theses_and_dissertations

Jankowski, K. L., Törnqvist, T. E., & Fernandes, A. M. (2017). Vulnerability of Louisiana's coastal wetlands to present-day rates of relative sea-level rise. *Nature Communications*, *8*, 14792. https://doi.org/10.1038/ncomms14792

Jelgersma, S. (1961). Holocene sea level changes in the Netherlands. *Mededelingen van de Geologische Stichting, Serie C*, *6*(7), 1–100.

Kaye, C. A., & Barghoorn, E. S. (1964). Late Quaternary sea-level change and crustal rise at Boston, Massachusetts, with notes on the autocompaction of peat. *Geological Society of America Bulletin*, *75*, 63–80. https://doi.org/10.1130/0016-7606(1964)75[63:lqscac]2.0.co;2

Kemp, A. C., Wright, A. J., Edwards, R. J., Barnett, R. L., Brain, M. J., Kopp, R. E., et al. (2018). Relative sea-level change in Newfoundland, Canada during the past ~3000 years. *Quaternary Science Reviews*, *201*, 89–110. https://doi.org/10.1016/j.quascirev.2018.10.012

Keogh, M. E., Kolker, A. S., Snedden, G. A., & Renfro, A. A. (2019). Hydrodynamic controls on sediment retention in an emerging diversion-fed delta. *Geomorphology*, *332*, 100–111. https://doi.org/10.1016/j.geomorph.2019.02.008

Keogh, M. E., & Törnqvist, T. E. (2019). Measuring rates of present-day relative sea-level rise in low-elevation coastal zones: A critical evaluation. *Ocean Science*, *15*, 61–73. https://doi.org/10.5194/os-15-61-2019

Khan, N. S., Horton, B. P., Engelhart, S., Rovere, A., Vacchi, M., Ashe, E. L., et al. (2019). Inception of a global atlas of sea levels since the Last Glacial Maximum. *Quaternary Science Reviews*, *220*, 359–371. https://doi.org/10.1016/j.quascirev.2019.07.016

Kolb, C. R., & Van Lopik, J. R. (1966). Depositional environments of the Mississippi River deltaic plain – Southeastern Louisiana. In M. L. Shirley (Ed.), *Deltas in their geologic framework* (pp. 17–61). Houston Geological Society.

Kolker, A. S., Dausman, A. M., Allison, M. A., Brown, G. L., Chu, P. Y., de Mutsert, K., et al. (2018). Rethinking the river. *Eos*, *99*. https://doi.org/10.1029/2018EO101169

Kolker, A. S., Goodbred, S. L., Jr., Hameed, S., & Cochran, J. K. (2009). High-resolution records of the response of coastal wetland systems to long-term and short-term sea-level variability. *Estuarine, Coastal and Shelf Science*, *84*, 493–508. https://doi.org/10.1016/j.ecss.2009.06.030

Kooi, H., Bakr, M., de Lange, G., den Haan, E., & Erkens, G. (2018). User guide to SUB-CR: A MODFLOW package for land subsidence and aquifer system compaction that includes creep. Deltares report 11202275-008. Retrieved from http://publications.deltares.nl/11202275_008.pdf

Kuecher, G. J., Chandra, N., Roberts, H. H., Suhayda, J. H., Williams, S. J., Penland, S. P., & Autin, W. J. (1993). Consolidation settlement potential in south Louisiana. In *Proceedings, 8th symposium on coastal and ocean management* (pp. 1197–1214).

Lorenzo-Trueba, J., Voller, V. R., Paola, C., Twilley, R. R., & Bevington, A. E. (2012). Exploring the role of organic matter accumulation on delta evolution. *Journal of Geophysical Research*, *117*, F00A02. https://doi.org/10.1029/2012jf002339

Mariotti, G., Elsey-Quirk, T., Bruno, G., & Valentine, K. (2020). Mud-associated organic matter and its direct and indirect role in marsh organic matter accumulation and vertical accretion. *Limnology & Oceanography*, *65*, 2626–2641. https://doi.org/10.1002/lno.11475

Marriner, N., Flaux, C., Morhange, C., & Kaniewski, D. (2012). Nile Delta's sinking past: Quantifiable links with Holocene compaction and climate-driven changes in sediment supply? *Geology*, *40*, 1083–1086. https://doi.org/10.1130/g33209.1

Marsh, P., Lesack, L. F. W., & Roberts, A. (1999). Lake sedimentation in the Mackenzie Delta, NWT. *Hydrological Processes*, *13*, 2519–2536. https://doi.org/10.1002/(sici)1099-1085(199911)13:16<2519::aid-hyp935>3.0.co;2-t

Mazzotti, S., Lambert, A., van der Kooij, M., & Mainville, A. (2009). Impact of anthropogenic subsidence on relative sea-level rise in the Fraser River delta. *Geology*, *37*, 771–774. https://doi.org/10.1130/g25640a.1

Meckel, T. A., ten Brink, U. S., & Williams, S. J. (2006). Current subsidence rates due to compaction of Holocene sediments in southern Louisiana. *Geophysical Research Letters*, *33*, L11403. https://doi.org/10.1029/2006gl026300

Miller, R. L., Fram, M. S., Fujii, R., Wheeler, G., & Wheeler, G. (2008). Subsidence reversal in a re-established wetland in the Sacramento-San Joaquin Delta, California, USA. *San Francisco Estuary and Watershed Science*, *6*. https://doi.org/10.15447/sfews.2008v6iss3art1

Milliman, J. D., & Haq, B. U. (Eds.). (1996). Sea-level rise and coastal subsidence: Causes, consequences, and strategies. In *Coastal systems and continental margins* (Vol. 2). Kluwer.

Minderhoud, P. S. J., Coumou, L., Erban, L. E., Middelkoop, H., Stouthamer, E., & Addink, E. A. (2018). The relationship between land use and subsidence in the Vietnamese Mekong delta. *Science of the Total Environment*, *634*, 715–726. https://doi.org/10.1016/j.scitotenv.2018.03.372

Morris, J. T., Barber, D. C., Callaway, J. C., Chambers, R., Hagen, S. C., Hopkinson, C. S., et al. (2016). Contributions of organic and inorganic matter to sediment volume and accretion in tidal wetlands at steady state. *Earth's Future*, *4*, 110–121. https://doi.org/10.1002/2015ef000334

Nadon, G. C. (1998). Magnitude and timing of peat-to-coal compaction. *Geology*, *26*, 727–730. https://doi.org/10.1130/0091-7613(1998)026<0727:matopt>2.3.co;2

Netherlands Standardization Institute (NEN). (2006). *NEN 6740: Geotechnics - TGB 1990 - Basic requirements and loads*. Publisher NEN.

Neubauer, S. C. (2008). Contributions of mineral and organic components to tidal freshwater marsh accretion. *Estuarine, Coastal and Shelf Science*, *78*, 78–88. https://doi.org/10.1016/j.ecss.2007.11.011

Nienhuis, J. H., Ashton, A. D., Edmonds, D. A., Hoitink, A. J. F., Kettner, A. J., Rowland, J. C., & Törnqvist, T. E. (2020). Global-scale human impact on delta morphology has led to net land area gain. *Nature*, *577*, 514–518. https://doi.org/10.1038/s41586-019-1905-9

Nienhuis, J. H., Törnqvist, T. E., & Esposito, C. R. (2018). Crevasse splays versus avulsions: A recipe for land building with levee breaches. *Geophysical Research Letters*, *45*, 4058–4067. https://doi.org/10.1029/2018gl077933

Nyman, J. A., Crozier, C. R., & Delaune, R. D. (1994). Roles and patterns of hurricane sedimentation in an estuarine marsh landscape. *Estuarine, Coastal and Shelf Science*, *40*, 665–679. https://doi.org/10.1006/ecss.1995.0045

Nyman, J. A., Delaune, R. D., & Patrick, W. H., Jr. (1990). Wetland soil formation in the rapidly subsiding Mississippi River Deltaic Plain: Mineral and organic matter relationships. *Estuarine, Coastal and Shelf Science*, *31*, 57–69. https://doi.org/10.1016/0272-7714(90)90028-p

Nyman, J. A., Walters, R. J., Delaune, R. D., & Patrick, W. H., Jr. (2006). Marsh vertical accretion via vegetative growth. *Estuarine, Coastal and Shelf Science*, *69*, 370–380. https://doi.org/10.1016/j.ecss.2006.05.041

Oppenheimer, M., Glavovic, B. C., Hinkel, J., van de Wal, R., Magnan, A. K., Abd-Elgawad, A., et al. (2019). Sea level rise and implications for low-lying islands, coasts and communities. In H.-O. Pörtner, D. C. Roberts, V. Masson-Delmotte, P. Zhai, M. Tignor, E. Poloczanska, et al. (Eds.), *IPCC special report on the ocean and cryosphere in a changing climate* (pp. 321–445). Cambridge University Press.

Paola, C., Twilley, R. R., Edmonds, D. A., Kim, W., Mohrig, D., Parker, G., et al. (2011). Natural processes in delta restoration: Application to the Mississippi Delta. *Annual Review of Marine Science*, *3*, 67–91. https://doi.org/10.1146/annurev-marine-120709-142856

Peduto, D., Giangreco, C., & Venmans, A. A. M. (2020). Differential settlements affecting transition zones between bridges and road embankments on soft soils: Numerical analysis of maintenance scenarios by multi-source monitoring data assimilation. *Transportation Geotechnics*, *24*, 100369. https://doi.org/10.1016/j.trgeo.2020.100369

Peduto, D., Huber, M., Speranza, G., Van Ruijven, J., & Cascini, L. (2017). DInSAR data assimilation for settlement prediction: Case study of a railway embankment in the Netherlands. *Canadian Geotechnical Journal*, *54*, 502–517. https://doi.org/10.1139/cgj-2016-0425

Penland, S., & Ramsey, K. E. (1990). Relative sea-level rise in Louisiana and the Gulf of Mexico: 1908-1988. *Journal of Coastal Research*, *6*, 323–342.

Peyronnin, N., Caffey, R., Cowan, J., Justic, D., Kolker, A., Laska, S., et al. (2017). Optimizing sediment diversion operations: Working group recommendations for integrating complex ecological and social landscape interactions. *Water*, *9*, 368. https://doi.org/10.3390/w9060368

Pons, L. J., Jelgersma, S., Wiggers, A. J., & De Jong, J. D. (1963). Evolution of the Netherlands coastal area during the Holocene. *Verhandelingen van het Koninklijk Nederlands Geologisch Mijnbouwkundig Genootschap, Geologische Serie*, *21*(2), 197–208.

Redfield, A. C. (1972). Development of a New England salt marsh. *Ecological Monographs*, *42*, 201–237. https://doi.org/10.2307/1942263

Reed, D. J. (2002). Sea-level rise and coastal marsh sustainability: Geological and ecological factors in the Mississippi Delta plain. *Geomorphology*, *48*, 233–243. https://doi.org/10.1016/s0169-555x(02)00183-6

Rieke, H. H., & Chilingarian, G. V. (1974). Compaction of Argillaceous Sediments. *Developments in sedimentology* (Vol. 16). Elsevier.

Rosen, T., & Xu, J. (2013). Recent decadal growth of the Atchafalaya River Delta complex: Effects of variable riverine sediment input and vegetation succession. *Geomorphology*, *194*, 108–120. https://doi.org/10.1016/j.geomorph.2013.04.020

Rosenheim, B. E., Roe, K. M., Roberts, B. J., Kolker, A. S., Allison, M. A., & Johannesson, K. H. (2013). River discharge influences on particulate organic carbon age structure in the Mississippi/Atchafalaya River System. *Global Biogeochemical Cycles*, *27*, 1–13. https://doi.org/10.1002/gbc.20018

Sanks, K. M., Shaw, J. B., & Naithani, K. (2020). Field-based estimate of the sediment deficit in coastal Louisiana. *Journal of Geophysical Research: Earth Surface*, *125*, e2019JF005389. https://doi.org/10.1029/2019jf005389

Shen, Z., Törnqvist, T. E., Mauz, B., Chamberlain, E. L., Nijhuis, A. G., & Sandoval, L. (2015). Episodic overbank deposition as a dominant mechanism of floodplain and delta-plain aggradation. *Geology*, *43*, 875–878. https://doi.org/10.1130/g36847.1

Shirzaei, M., Freymueller, J., Törnqvist, T. E., Galloway, D. L., Dura, T., & Minderhoud, P. S. J. (2021). Measuring, modelling and projecting coastal land subsidence. *Nature Reviews Earth & Environment*, *2*, 40–58. https://doi.org/10.1038/s43017-020-00115-x

Stanley, D. J., Warne, A. G., & Dunbar, J. B. (1996). Eastern Mississippi Delta: Late Wisconsin unconformity, overlying transgressive facies, sea level and subsidence. *Engineering Geology*, *45*, 359–381. https://doi.org/10.1016/s0013-7952(96)00022-1

Steyer, G. D., Sasser, C. E., Visser, J. M., Swenson, E. M., Nyman, J. A., & Raynie, R. C. (2003). A proposed coast-wide reference monitoring system for evaluating wetland restoration trajectories in Louisiana. *Environmental Monitoring and Assessment*, *81*, 107–117. https://doi.org/10.1007/978-94-017-0299-7_11

Syvitski, J. P. M., Kettner, A. J., Overeem, I., Hutton, E. W. H., Hannon, M. T., Brakenridge, G. R., et al. (2009). Sinking deltas due to human activities. *Nature Geoscience*, *2*, 681–686. https://doi.org/10.1038/ngeo629

Syvitski, J. P. M., Vörösmarty, C. J., Kettner, A. J., & Green, P. (2005). Impact of humans on the flux of terrestrial sediment to the global coastal ocean. *Science*, *308*, 376–380. https://doi.org/10.1126/science.1109454

Tam, C.-Y., Zong, Y., bin Hassan, K., bin Ismal, H., binti Jamil, H., Xiong, H., et al. (2018). A below-the-present late Holocene relative sea level and the glacial isostatic adjustment during the Holocene in the Malay Peninsula. *Quaternary Science Reviews*, *201*, 206–222. https://doi.org/10.1016/j.quascirev.2018.10.009

Tamura, T., Saito, Y., Sieng, S., Ben, B., Kong, M., Sim, I., et al. (2009). Initiation of the Mekong River delta at 8 ka: Evidence from the sedimentary succession in the Cambodian lowland. *Quaternary Science Reviews*, *28*, 327–344. https://doi.org/10.1016/j.quascirev.2008.10.010

Teatini, P., Tosi, L., & Strozzi, T. (2011). Quantitative evidence that compaction of Holocene sediments drives the present land subsidence of the Po Delta, Italy. *Journal of Geophysical Research*, *116*, B08407. https://doi.org/10.1029/2010jb008122

Temmerman, S., & Kirwan, M. L. (2015). Building land with a rising sea. *Science*, *349*, 588–589. https://doi.org/10.1126/science.aac8312

Törnqvist, T. E., Cahoon, D. R., Morris, J. T., & Day, J. W. (2021). Coastal wetland resilience, accelerated sea-level rise, and the importance of timescale. *AGU Advances*, *2*, e2020AV000334.

Törnqvist, T. E., Jankowski, K. L., Li, Y.-X., & González, J. L. (2020). Tipping points of Mississippi Delta marshes due to accelerated sea-level rise. *Science Advances*, *6*, eaaz5512.

Törnqvist, T. E., Wallace, D. J., Storms, J. E. A., Wallinga, J., Van Dam, R. L., Blaauw, M., et al. (2008). Mississippi Delta subsidence primarily caused by compaction of Holocene strata. *Nature Geoscience*, *1*, 173–176.

Toscano, M. A., González, J. L., & Whelan, K. R. T. (2018). Calibrated density profiles of Caribbean mangrove peat sequences from computed tomography for assessment of peat preservation, compaction, and impacts on sea-level reconstructions. *Quaternary Research*, *89*, 201–222. https://doi.org/10.1017/qua.2017.101

Turner, R. E. (1997). Wetland loss in the Northern Gulf of Mexico: Multiple working hypotheses. *Estuaries*, *20*, 1–13. https://doi.org/10.2307/1352716

Turner, R. E., Swenson, E. M., & Milan, C. S. (2002). Organic and inorganic contributions to vertical accretion in salt marsh sediments. In M. P. Weinstein & D. A. Kreeger (Eds.), *Concepts and controversies in tidal marsh ecology* (pp. 583–595). Kluwer Academic Publishers.

Van Asselen, S. (2011). The contribution of peat compaction to total basin subsidence: Implications for the provision of accommodation space in organic-rich deltas. *Basin Research*, *23*, 239–255. https://doi.org/10.1111/j.1365-2117.2010.00482.x

Van Asselen, S., Erkens, G., Stouthamer, E., Woolderink, H. A. G., Geeraert, R. E. E., & Hefting, M. M. (2018). The relative contribution of peat compaction and oxidation to subsidence in built-up areas in the Rhine-Meuse delta, The Netherlands. *Science of the Total Environment*, *636*, 177–191. https://doi.org/10.1016/j.scitotenv.2018.04.141

Van Asselen, S., Karssenberg, D., & Stouthamer, E. (2011). Contribution of peat compaction to relative sea-level rise within Holocene deltas. *Geophysical Research Letters*, *38*, L24401. https://doi.org/10.1029/2011gl049835

Van Asselen, S., Stouthamer, E., & van Asch, T. W. J. (2009). Effects of peat compaction on delta evolution: A review on processes, responses, measuring and modeling. *Earth-Science Reviews*, *92*, 35–51. https://doi.org/10.1016/j.earscirev.2008.11.001

Van de Plassche, O. (1982). Sea-level change and water-level movements in the Netherlands during the Holocene. *Mededelingen Rijks Geologische Dienst*, *36*, 1–93.

Van de Plassche, O., Bohncke, S. J. P., Makaske, B., & Van der Plicht, J. (2005). Water-level changes in the Flevo area, central Netherlands (5300–1500 BC): Implications for relative mean sea-level rise in the Western Netherlands. *Quaternary International*, *133–134*, 77–93. https://doi.org/10.1016/j.quaint.2004.10.009

Van der Deijl, E. C., van der Perk, M., & Middelkoop, H. (2018). Establishing a sediment budget in the newly created "Kleine Noordwaard" wetland area in the Rhine-Meuse delta. *Earth Surface Dynamics*, *6*, 187–201. https://doi.org/10.5194/esurf-6-187-2018

Van der Meijs, R. C. J. (2015). Increasing the reliability of settlement predictions: A Bayesian approach (Master's thesis). Technische Universiteit Delft. Retrieved from Technische Universiteit Delft Institutional Repository http://resolver.tudelft.nl/uuid:e977cc50-39d7-4ab7-a8c5-c7501dfdc03c

Visschedijk, M. A. T., & Trompille, V. (Eds.). (2009). Verification. *MSettle version 8.2: Embankment design and soil settlement prediction* (pp. 331–429). Deltares.

Vörösmarty, C. J., Meybeck, M., Fekete, B., Sharma, K., Green, P., & Syvitski, J. P. M. (2003). Anthropogenic sediment retention: Major global impact from registered river impoundments. *Global and Planetary Change*, *39*, 169–190. https://doi.org/10.1016/S0921-8181(03)00023-7

Walker, J. S., Kopp, R. E., Shaw, T. A., Cahill, N., Khan, N. S., Barber, D. C., et al. (2021). Common Era sea-level budgets along the U.S. Atlantic coast. *Nature Communications*, *12*, 1841. https://doi.org/10.1038/s41467-021-22079-2

Weston, N. B. (2014). Declining sediments and rising seas: An unfortunate convergence for tidal wetlands. *Estuaries and Coasts*, *37*, 1–23. https://doi.org/10.1007/s12237-013-9654-8

Xu, K., Bentley, S. J., Day, J. W., & Freeman, A. M. (2019). A review of sediment diversion in the Mississippi River Deltaic Plain. *Estuarine, Coastal and Shelf Science*, *225*, 106241. https://doi.org/10.1016/j.ecss.2019.05.023

Yang, Z., Wang, H., Saito, Y., Milliman, J. D., Xu, K., Qiao, S., & Shi, G. (2006). Dam impacts on the Changjiang (Yangtze) River sediment discharge to the sea: The past 55 years and after the Three Gorges Dam. *Water Resources Research*, *42*, W04407. https://doi.org/10.1029/2005wr003970

Zhang, J. Z., Huang, H., & Bi, H. (2015). Land subsidence in the modern Yellow River Delta based on InSAR time series analysis. *Natural Hazards*, *75*, 2385–2397. https://doi.org/10.1007/s11069-014-1434-7

Zoccarato, C., & Da Lio, C. (2021). The Holocene influence on the future evolution of the Venice Lagoon tidal marshes. *Communications Earth & Environment*, *2*, 77. https://doi.org/10.1038/s43247-021-00144-4

Zoccarato, C., Minderhoud, P. S. J., & Teatini, P. (2018). The role of sedimentation and natural compaction in a prograding delta: Insights from the mega Mekong delta, Vietnam. *Scientific Reports*, *8*, 11437. https://doi.org/10.1038/s41598-018-29734-7

Zoccarato, C., & Teatini, P. (2017). Numerical simulations of Holocene salt-marsh dynamics under the hypothesis of large soil deformations. *Advances in Water Resources*, *110*, 107–119. https://doi.org/10.1016/j.advwatres.2017.10.006

Zoccarato, C., Törnqvist, T. E., Teatini, P., & Bridgeman, J. G. (2020). A shallow compaction model for Holocene Mississippi Delta sediments. *Proceedings of the International Association of Hydrological Sciences*, *382*, 565–570. https://doi.org/10.5194/piahs-382-565-2020